Uncertainty in hardness measurement

Laurence Brice, Francis Davis, and Andrew Crawshaw

April 2003

April 2003

Uncertainty in hardness measurement

Laurence Brice, Francis Davis, and Andrew Crawshaw
Centre for Mechanical and Acoustical Metrology
National Physical Laboratory
Queens Road
Teddington
Middlesex
TW11 0LW

Abstract

This report details work into the factors contributing to uncertainty in measured hardness, including a literature review of the factors contributing to uncertainty in hardness metrology, and their complex interactions. In many areas, contradictions existed and highlighted the need for further research. The effects of the indenter characteristics were identified as major factors contributing to the uncertainty in measured hardness, so work was done to determine these influences.

This work concentrated on the main characteristics of Vickers and Rockwell indenters, investigating how they affected the measured hardness across a range of hardnesses.

With the results obtained, the effects caused by the different characteristics were evaluated and the more significant were identified.

The work described was carried out under Deliverable 2.3.5 of the National Measurement System's Mass Programme 1999-2002, funded by the Department of Trade and Industry.

ISSN 1369-6785

National Physical Laboratory
Teddington, Middlesex, United Kingdom TW11 0LW

Approved on behalf of Managing Director, NPL,
by Dr R Preston, Authorised by Head of NPL Material Centre

CONTENTS

TABLES

FIGURES

1. Background

Hardness is a measure of a material's resistance to local deformation caused by an indentation from a hard body. Unlike most other material properties, hardness is not a unique property, but is dependent on the nature of the test employed. There are a number of different indentation hardness tests widely used with many common features. However, the particular indentation force, or forces, applied by each test differ, as does the dynamics of the indentation process. Due to these differences there are no units of hardness upon which to base a standardised scale. Traceability in hardness is to the test method employed, and relationships between the various scales and test methods are not exact.

In the past, hardness measurement precluded procedures for defining fundamental metrological units for comparing standards between nationally accredited laboratories, and the method for the dissemination of hardness scales was by the comparison of calibrated hardness blocks. Ideally, calibration machines built to the specification defined in the specific hardness standard should ensure that hardness blocks calibrated in accredited laboratories are identical. In practice, this is not the case. In addition, some accredited laboratories give scales of hardness which are unstable, and calibrated test blocks purchased at different time intervals can provide different hardnesses readings due to their deterioration over time. Such indirect verification and comparison of hardness scales are no longer acceptable to the metrologist and a reliable system of direct verification of hardness standards is required.

Direct verification requires the determination of the following uncertainties: (i) the standard hardness machine, (ii) the characteristics of the standard grade indenter, and, to ensure a robust metrological relationship between direct and indirect calibration, (iii) the measurement of the indentation, and (iv) the metallurgy of the test block.

The most common scales in indentation hardness testing in industry are Brinell, Vickers, and Rockwell. These were developed to meet the needs of the foundry, metallurgical, and engineering industries respectively. Standards exist [1, 2 and 3] which define the fundamentals of the methodology of individual hardness tests and the preferred scales. NPL is responsible for the re-establishment of the UK national hardness scales, as shown in Table 1.

Table 1. UK hardness scales supported.

	Scales	Nominal Force (N)
Brinell	HB10/3000	30 000
	HB10/1000	10 000
	HB5/750	7 500
	HB2.5/187.5	1 900
Rockwell	HRB	100 to 900
	HRC	100 to 1 500
Superficial Rockwell	HR30N, HR30T	100 and 300
Vickers	HV10	100
	HV30	300

To understand the uncertainty contribution of the individual measurand a critical literature review has been carried out. The information and knowledge gained will be applied to calculate the uncertainty budget for the UK national hardness standards.

2. Uncertainties in Hardness Measurement - A Literature Review

2.1 The Influence of the Machine

The "true value" of hardness is achieved by the "ideal operator" [4], using the "ideal standards hardness calibration machine" with the "ideal indenter" and working to the standards [1, 2 and 3] without any error. In practice, it is impossible to realise the true value of the hardness scale, because the hardness machine and indenter cannot be manufactured and calibrated without some error. However, by controlling and reducing such errors of the reference standards, both random and systematic errors and their uncertainty contribution to the hardness scales can be minimised.

The influence of the standards hardness calibration machine includes: (i) the test force, (ii) the test cycle time, and (iii) the magnitude of penetration of the indenter.

Barbato et al [5] have investigated the effect of the test indentation cycle on the uncertainties of Rockwell hardness measurement. The experimental parameters describing the indentation cycle are shown in Figure 1. The most important parameters include the approach velocity (V_0), the velocity during the initial preliminary force stage and the initial part of the loading stage (V_1), the velocity of the last part of the loading stage (V_{LR}), the pre-load dwell time (T_P), the major load increment time (T_L) and the total load dwell time (T_M). In the investigation, parameters were either evaluated singularly (V_0 and T_M) or jointly (V_1 with T_P and V_{LR} with T_L).

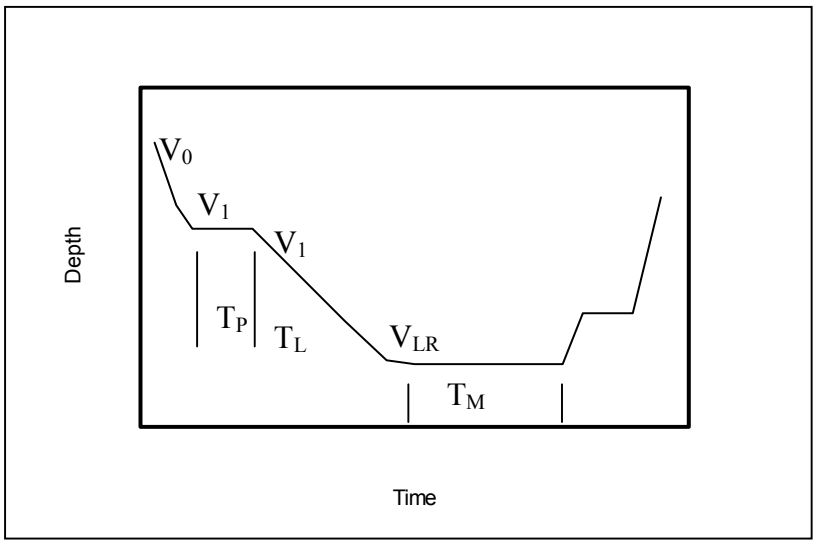

Figure 1. Main parameters of the indentation cycle

The results of the Barbato et al investigation on contribution to uncertainty are summarised below:

- The effect of the approach velocity (V_0) was minimal. Only at low hardness and approach velocities of 0.1 – 1.0 mm s^{-1} was there any significant effect.
- The effect of total load dwell time (T_M) was dependent upon the creep characteristics of the test block material. Creep characteristics have previously been studied for different materials and tolerances specified. A proposal, by Barbato et al [6] was that the dwell time should be defined by the creep characteristics of the material; this would improve the accuracy of hardness measurement. For calibration machines with a 0.1 μm resolution, a dwell time of 10 s was recommended whilst, for efficiency in the workshop, hardness machine of a 0.5 μm resolution could use a reduced dwell time of about 4 s.
- The combined effect of velocity (V_1) and the pre-load dwell time (T_P) can be expressed as:

$$\Delta HRC = A + B \cdot \ln(T_P) + C \cdot \ln(V_1) + D \cdot \ln(T_P) \cdot \ln(V_1)$$

  Using the derived regression coefficients, then the calculated ΔHRC value was ± 0.35 HRC at 25 HRC, ± 0.25 HRC at 40 HRC, and ± 0.15 HRC at 60 HRC. This compares with the ISO standard quoted for T_P and over a reasonable variation of V_1 (not defined in the standard) of ± 0.2 HRC and less than ± 0.1 HRC at 60 HRC. The contribution of V_1 was considered to be lower than ± 0.1 HRC.

- The effect of velocity (V_{LR}) during the last part of the loading stage and the loading time (T_L) were the most difficult to separate. Limiting the velocity to less than 0.1 mm s^{-1}, and using multiple regression analysis, hardness variations were independent of the loading time at 40 HRC, whereas the effect of velocity was significant at both the 25 HRC and 60 HRC values. The effect of V_{LR} was suggested to be attributable to the block metallurgy.

The main conclusion of Barbato et al's investigation was that for hardness calibration machines there is a necessity to define an operating test cycle envelope to minimise the effect on uncertainty. Further, that this working envelope may not be the same as used in a workshop environment although a relationship between the conditions needs to be determined.

Recent revision of the Rockwell hardness standard test method [2] allows the use of hardmetal (tungsten carbide) balls for all Rockwell scales that use ball indenters. This revised standard also suggested that for the next revision, the standard test forces should be changed from Kilogram-force based values to Newton-based values, i.e. for the Rockwell HRC scale the total force of 1.471 kN (150 kgf) would become 1.5 kN. These changes to Rockwell hardness measurement have been investigated by NIST [8]. The force revision affects the Rockwell hardness test in two ways: (i) a shift in the hardness measurement due to the change in the applied force, and (ii) modification of deadweight hardness machines. The proposed changes in force levels are shown in Table 2. Also included, in the table, are the ASTM and ISO tolerances and, as can be seen, the changes are in some cases outside the allowable force tolerances.

Table 2. Present and proposed Rockwell test forces.

Present force (N), (Approx kgf)	Proposed force (N)	Change in force (N)	ASTM tolerance (N)	ISO tolerance (N)x
29.42 (3)	30	+ 0.58	± 0.589	± 0.588
98.07 (10)	100	+ 1.93	± 1.96	± 1.96
147.1 (15)	150	+ 2.9	± 0.981	± 1.471
294.2 (30)	300	+ 5.8	± 1.961	± 2.942
441.3 (45)	450	+ 8.7	± 2.943	± 4.413
588.4 (60)	600	+ 11.6	± 4.41	± 5.88
980.7 (100)	1000	+ 19.3	± 4.57	± 9.81
1471 (150)	1500	+ 29.0	± 8.83	± 14.71

NIST's investigation of the Rockwell HRA scale showed that the increase in preliminary force increased the indentation depth, resulting in a reduction of the Δdepth value used for the calculation of the Rockwell hardness value and an apparent increased hardness. When the total force value was increased, and the additional force removed, returning to the preliminary force level, the increased indentation depth was maintained. This increase in indentation depth increased the Δdepth value, which resulted in an apparent lower hardness value. This investigation showed that re-defining the force level will require the relationship between the applied forces and hardness values for each Rockwell scale to be re-established and their uncertainties assessed. Any advantage from re-defining the forces would be outweighed by the associated costs of any modification to the deadweight machines. In contrast, the use of a hardmetal ball offered potential advantages and improvement in Rockwell hardness measurement uncertainties. The higher hardness of a tungsten carbide ball will be less likely to cause flattening of the indenter with repeated use and therefore give improved repeatability, albeit that the hardness value may differ due to changes in indenter/test block interface and further investigation is required.

Joint research by the Italian and German NMIs [6] showed the influence of creep in the test block on the measured hardness of the Superficial Rockwell HR45N scale. Tests were performed on two pairs of hardness blocks, with rated hardness values of 20 HRC and 35 HRC, from two manufacturers. The total force dwell time was varied from 2 - 30 s at three-second intervals. At each interval, the mean hardness was calculated from three measurements. The results are shown in Figures 2 and 3.

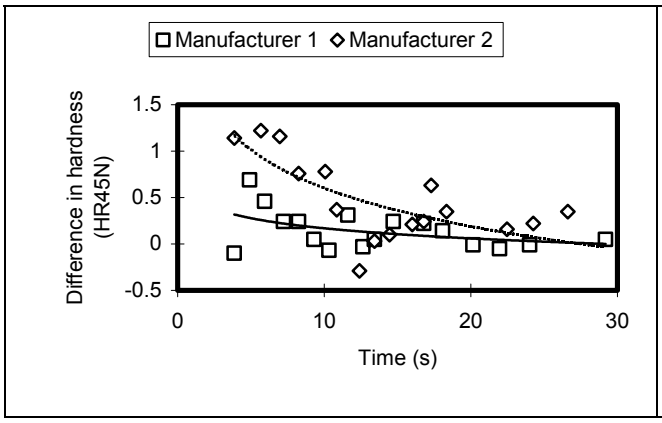

Figure 2. Hardness variation caused by total force dwell time at 20 HRC.

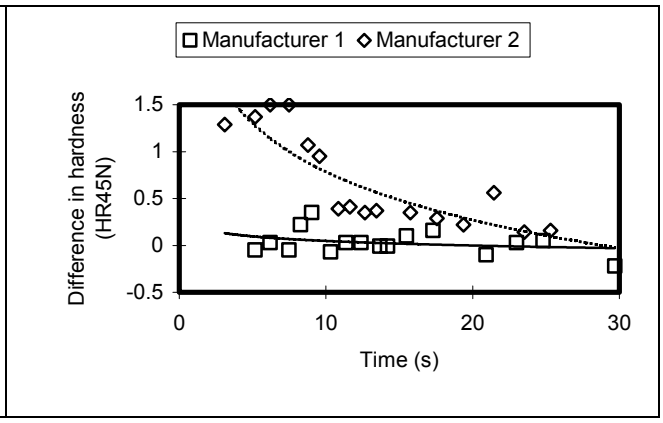

Figure 3. Hardness variation caused by total force dwell time at 35 HRC.

The results showed that the creep effect due to dwell time, within the tolerances of 2 – 4 s accepted by ISO and EN standards, could produce very significant differences in the measured hardness. Increasing the dwell times to a minimum of 10 s reduced the problem for test block Manufacturer 1, although not for Manufacturer 2. Further work [9] investigating the creep of hardness test blocks showed different trends for different materials of the same hardness. This was attributed to differences in slip systems controlling the deformation process and the friction of the indenter.

Ishida [10] has also investigated the effect of indenter velocity on the measured hardness; the results are shown in Figure 4.

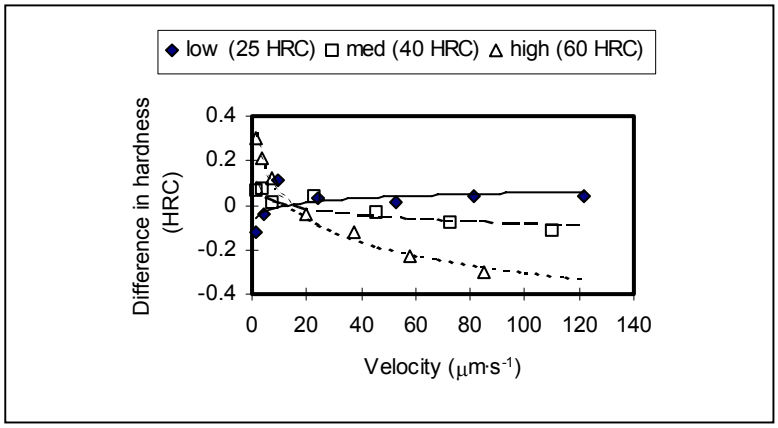

Figure 4. Differences in Rockwell HRC measurement due to indenter velocity.

The 60 HRC block, at low velocity, showed a similar significant dependency to that reported by Barbato et al [5] whereas for the 25 HRC and 40 HRC the effect of velocity was less apparent. Further, the results showed that at 25 HRC hardness increased with velocity up to about 10 μm s^{-1} whereas, the reverse was observed for the 40 HRC test block. For all test block at velocities between 80 and 100 μm s^{-1} the effect diminished, and Ishida recommends that this velocity range be included in the standard. Similar to the conclusions of Barbato et al [5], the test block

metallurgy was considered responsible and, in particular, the strain hardening characteristics of the test block.

Ishida [10] has also carried out a similar investigation to the joint German/Italy study [6] to characterise the influence of both the loading and holding time on the deformation process. This investigation was carried out using the NRLM Rockwell standards machine and investigated three hardness levels, 20, 40, and 60 HRC and at three loading or holding test times (3, 10 and 25 s). Figure 5 shows the effect of loading (a and b) and un-loading (c) times during the three stages of the Rockwell test. The results are expressed as a difference in indenter depth, relative to the mean measurement at 10 s.

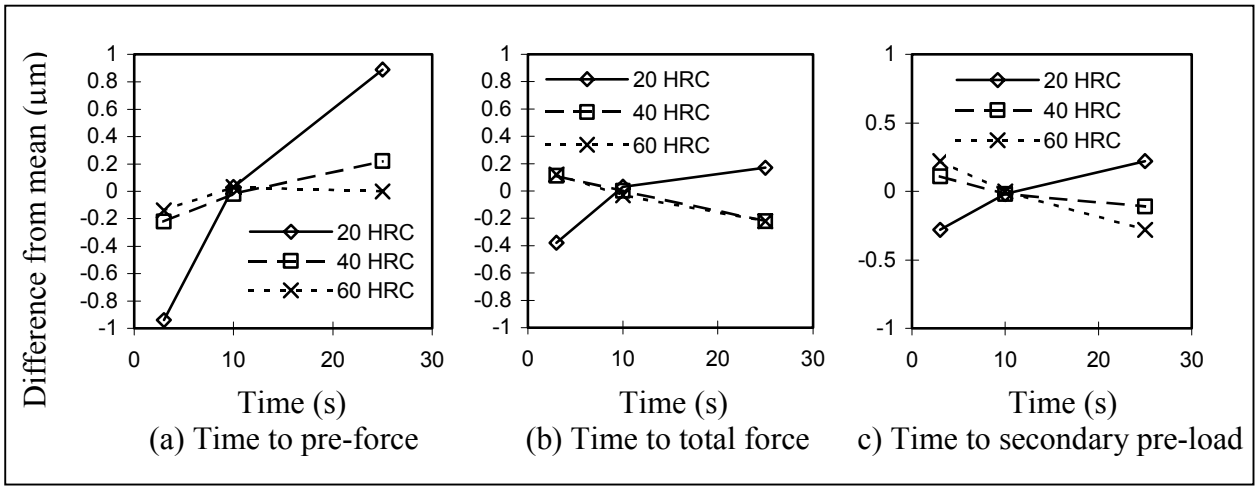

Figure 5. The effect of loading and un-loading time on indentation depth.

The results showed that during the application of the pre-force, increasing the loading time to 10 s increased the indentation depth, although the rate decreased with the hardness of the test block. For the 20 HRC test block a further increase in loading time (i.e. further reduction of the indenter velocity) resulted in a greater indentation depth and apparent softening of the test block, whereas the 60 block HRC block revealed no further increase in the indentation depth. The application of the total force and secondary pre-force resulted in an increased apparent hardness of the 40 and 60 HRC test blocks with increasing time; for the 20 HRC block the opposite trend was observed.

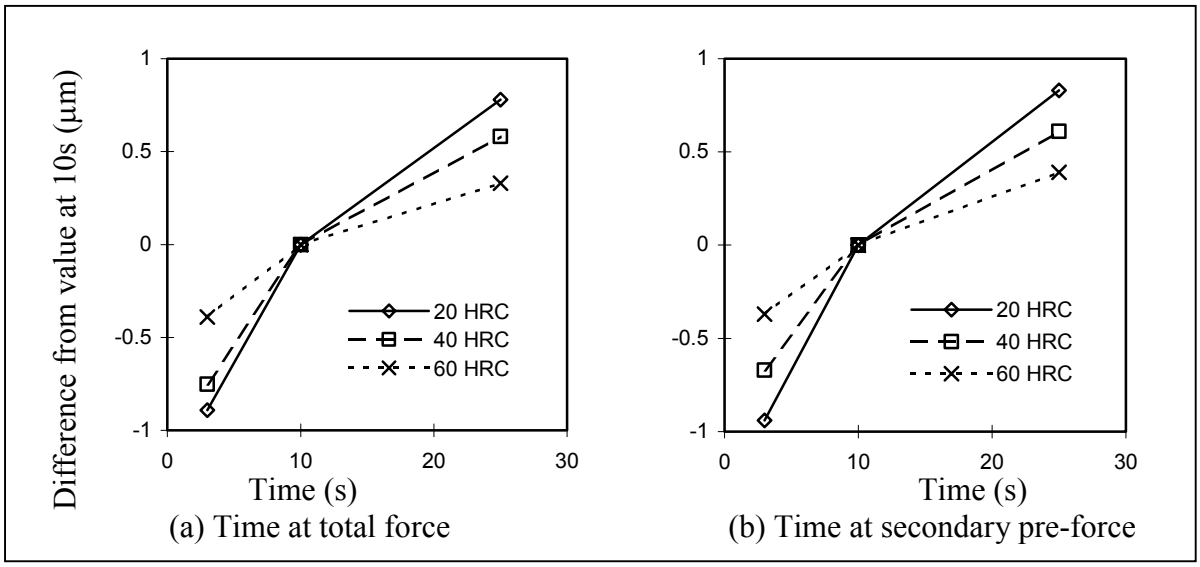

Figure 6. Effect of holding time at the total force and secondary preliminary force condition on indentation depth

Figure 6, the effect of holding time, at both total force and secondary pre-force, showed that as the holding time was increased then the indentation depth increased, the apparent increase in indentation depth decreased the harder the test block.

Ishida [10] explained his observations by consideration of the deformation process; when the force application time period was short the material deformation rate followed the indenter's movement. This delay in the material's deformation was overcome during the force holding periods due to creep adding to the deformation process. Conversely, if the force application periods were increased, resulting in a reduction of the indenter's velocity, only creep occurred during the holding period. The rate of application of force and holding time will be different for each material and hardness level. This more extensive study of Ishida [10] concluded, similar to the work of Barbato et al [5 and 6], the inter-dependency of indenter velocity and time at each loading condition and the necessity to define an operating test cycle envelope that minimised the effects of the loading cycle on uncertainty. Ishida also makes a similar point that this test cycle envelope may be different in the calibration standards laboratory and the workshop, but a relationship between the test environments needs to be established.

In an attempt to resolve the influence of the test cycle on hardness uncertainties of the Rockwell hardness test, Koike and Ishida [11] have applied a noise factor orthogonal array design (NFOAD) of Taguchi Methods [12]. An advantage of this approach is the ability to reduce the many variables in one series of experiments. Regression analysis of experimental data provided the sensitivity coefficient (β) as a function of the applied test conditions and parameters, whilst for parameters not

considered in the experimental design, the estimated standard deviation (σ) was used. Table 3 shows the results of their statistical analysis.

Table 3. Example of uncertainty estimation based on NFOAD experiments.

Error source	β	σ	$u = \lvert \beta\sigma \rvert$ (HRC)	u^2 (HRC^2)
Reference load	0.06002(HRC/N)	1.132(N)	0.0679	0.00461
Test load	-0.02506(HRC/N)	14.710(N)	0.3686	0.13587
Holding time	-0.0108(s)	1.1547(s)	0.0208	0.00043
Reproducibility			0.1767	0.03124
Test block			0.1000	0.01000
Combined uncertainty u_c			0.43 (HRC)	

Work by Yamamoto and Yamamoto [13] studied the influence of indentation load duration in Vickers hardness. Their investigation considered a range of test block materials, including steel and ceramics, over a time range of 2 – 1 000 s. Figure 7 shows the average of five hardness values, measured at either HV 5 or HV 10.

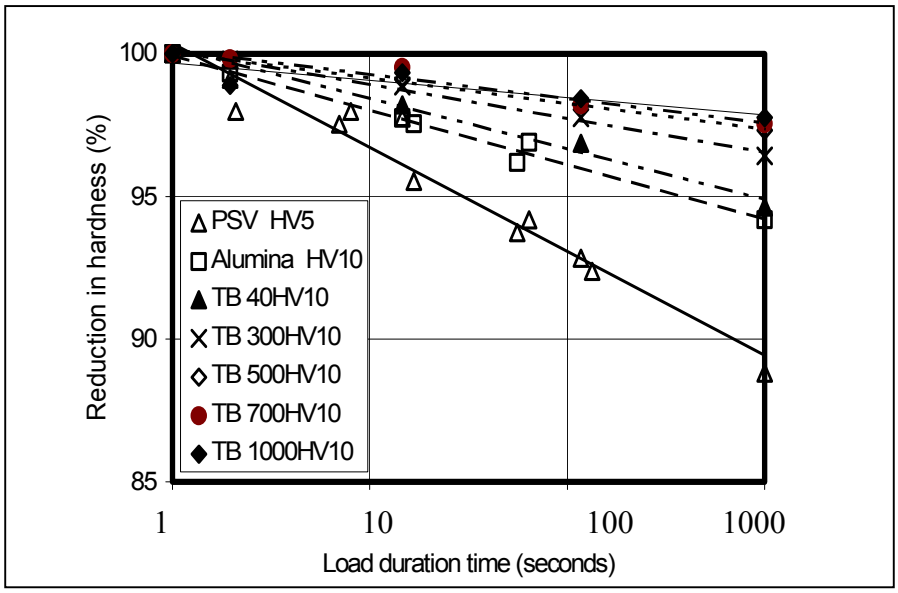

Figure 7. Effect of load duration time on Vickers hardness

The results indicated an apparent logarithmic reduction in hardness with time, and that the rate of decline decreased with increasing hardness of the test blocks. Yamamoto attributed this apparent softening to the creep deformation of the test block material, although also considered was the elastic recovery of the test block and that possibly the elasticity of the indenter played a role. Not surprisingly, the

trend of these results appears similar to those for the effect of dwell time on apparent Rockwell hardness, as reported by Barbato et al [5 and 6] and Ishida [10].

Further work by Yamamoto and Yamamoto [14] investigated the influence of loading velocity on Vickers hardness (Figure 8).

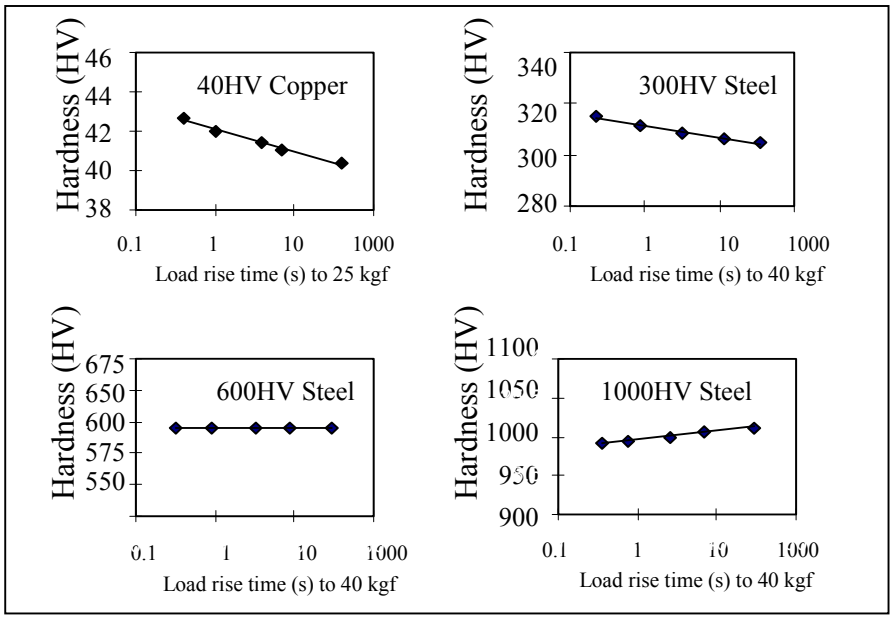

Figure 8. The effect of loading time on Vickers hardness

Their results showed for the soft copper and the 300 HV steel that as the indenter penetration time was reduced (i.e. the velocity increased) the apparent hardness of the material decreased, although the rate of hardness reduction decreased with the increasing hardness. For the 600 HV steel, hardness was not influence by loading velocity whilst, for the hardest 1000 HV steel a slight increase in hardness was observed with increased loading velocity. In general, this trend was similar to that shown in Figure 7. Yamamoto et al provide no explanation for their results. At low hardness, 40 HV and 300 HV, the trend, in general, appears similar to that reported for Rockwell hardness testing by both Barbato et al [5 and 6] and Ishidi [10]. However, for the harder steels, 600 HV and 1000 HV, the effect of indenter velocity on hardness was not as apparent, compare results with that shown in Figure 4 for the 60 HRC steel. A possible explanation is the shape of the indenters on the dynamics of the indentation process.

A survey of Vickers machines was carried out by NPL [15] in 1984. The survey investigated the indirect verification of 15 commercial hardness machines and compared the results with the two NPL standard Vickers hardness machines; all the commercial machines were regularly maintained. The survey considered both HV 10 and HV 30 scales at nominal block hardness's of 150, 300 and 800 HV. The results showed excellent repeatability, but over half the values exceeded the 2 % tolerance. Correction of the results for systematic errors and for magnification of the microscope used for measuring the diagonal reduced the uncertainty of measurement to within the 2 % tolerance. No single cause for the systematic errors

was identified other than the conclusion that it would appear to be the measuring system used by the operator. Over half the commercial measuring systems exceeded the allowable ± 0.5 % magnification error.

2.2 The Influence of the Indenter

The main causes of differences in hardness measurement are due to indenter effects. The replacement of an indenter represents a new hardness scale as illustrated by the replacement of Rockwell indenters by NPL [16] and the Establishment Technique Central de l'Armemant (ETCA) in France [17]. The contribution to hardness uncertainty of a Rockwell diamond indenter is due primarily to the geometry of the indenter, i.e. the 120 ° cone angle and the tangential blend to the spherical tip of 200 μm radius. It has been shown that, provided the same diamond indenter was used, machines of quite different designs were capable of giving the same hardness scales. Whereas, if more than one indenter was involved, limited agreement between machines was observed [18]. This was attributed to the poor traceability in characterising indenters and, therefore, poor reproducibility when changing indenters. In addition, continuous use of an indenter can cause a drift in the characteristics of an indenter and thus cause a change in the hardness scale [19].

It is therefore necessary to use a metrological approach to identify the important characteristics of an indenter and their influence on changes in hardness scales. Transparency is essential for all accredited laboratories involved in calibration metrology and certification [20]. This means that procedures, techniques and reference standards used to establish a hardness scale must be documented such that they can be reproduced in other standards laboratories.

An extensive investigation by NPL [21] was carried out to investigate the influence of indenter morphology on the performance of Rockwell HRC, HRA and HR 30 N scales. The results of the effect of indenter radius and cone angle are shown in Figures 9 and 10.

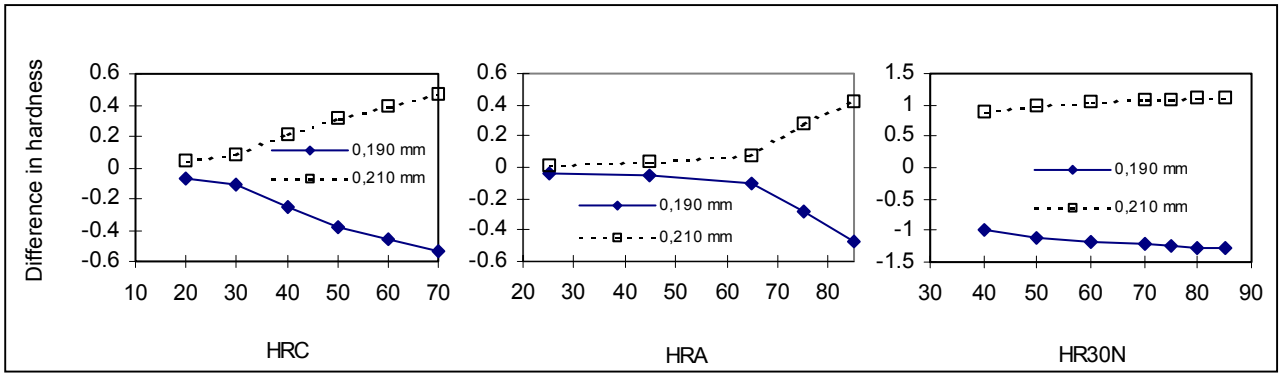

Figure 9. The effect of Rockwell indenter radius on measured hardness

The effect of indenter radius was similar for all scales, a reduction in the radius resulted in an apparent softening of the test block, whilst an increase in the radius

resulted in an apparent increased hardness, and that the indenter radius was more critical for the harder test blocks. Greater differences were observed for the superficial hardness test, this was suggested to be due to the limited indenter penetration.

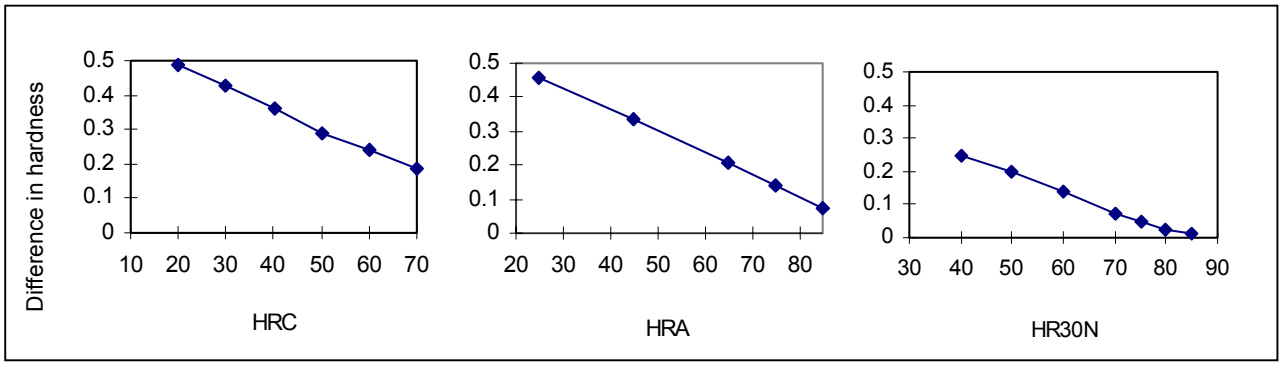

Figure 10. The effect of a ±0.35% variation in Rockwell cone angle on measured hardness

Surprisingly, the effect of a ±0.35° variation in the 120° cone angle on measured hardness was the same. Wood and Cotter [21] offered little explanation other than the hardness variation was related to the depth of indenter penetration, and that at 120° the maximum penetration occurred. This explanation would also account for the reduction in hardness variation with: (i) with increasing hardness of the test blocks, and (ii) with reduction in applied force in the order HRC, HRA and HR 30 N. The authors of this report recommend further studies to investigate the influence of the reduced tolerances of indenter radius and cone angle for both calibration and standard Rockwell indenters on variation in hardness measurement and contribution to hardness uncertainty.

Investigations by NIST [22, 23 and 24] have identified the key characteristics of Rockwell diamond indenters and concluded that both geometric and non-geometric properties affect the hardness performance. The geometric properties include the mean tip radius, the maximum and minimum radius, profile peak and valley deviations, the mean cone angle, the maximum and minimum cone angle, the cone flank straightness, the holder axis alignment, the surface roughness, and surface defects. The non-geometric properties include the mechanical properties of the diamond and the soldering of the diamond prism into the holder. NIST have proposed geometric tolerance and performance uniformity of grades of Rockwell indenters dependent on its application. The geometric tolerance and contribution to uncertainty of these graded Rockwell indenters are shown in Table 4.

Table 4. Technical requirements for three grades of Rockwell Indenters and NIST expanded measurement uncertainties.

Microform Geometric Characteristics	Tolerance			NIST Expanded Measurement Uncertainty (95%)
	Working Grade (ISO/716-1986, ASTM E18-94, EN 10109-2:1994)	Calibration Grade (ISO/674-1998, ASTM E18-94 EN 10109-3 1994)	Standard Grade (NIST Proposal)	
1. Spherical Radius				
1a. Least square mean	200 ± 10 μm	200 ± 5 μm	200 ± 2.5 μm	± 0.4 μm
1b.Maximum variation	200 + 15 μm	200 + 7 μm	200 + 3.5 μm	
1c. Profile deviation	± 2 μm [1,2], 4 μm [3]	± 2 μm [1,2], 2 μm [3]	± 0.25 μm	
2. Cone Angle				
2a. Least square mean	120 ° ± 3.5 °	120 ° ± 0.1 °	120 ° ± 0.05 °	± 0.01 °
2b.Maximum variation	< 1 μm [1,3]	120 ° ± 0.17 ° [1,3]	120 ° ± 0.08 °	
2c.Cone flank straightness		< 0.5 μm [1,3]	< 0.25 μm	
3. Holder Axis Alignment	± 0.5 °	± 0.3 °	± 0.15 °	± 0.025 °
4. Surface Finish				
4a. Mean roughness			R_a < 0.004 μm	
4b.Maximum roughness			$R_{a\,(max)}$ < 0.005 μm	
Performance Uniformity Requirements	± 0.8 HRC [1] ± 0.8 HR [3] with respect to a standard indenter	± 0.4 HRC [1] ± 0.4 HR [3] with respect to a standard indenter	± 0.15 HRC within a group of geometrically qualified standard indenters	

[1] Specified in ISO Standard: [2] Specified in ASTM Standard: [3] Specified in EN Standard, the performance uniformity is tested at 20 HRC, 55 HRD, 43 HR45N and 92 HR15N.

The geometric tolerances for a standard grade indenter are designed to give a performance uniformity range of ±0.15 HRC, this being close to the combined random variation range of a standard hardness machine and standard test block. Indirect verification of the diamond indenter must therefore include these variations in developing any uncertainty budget. NIST have reported the repeatability of hardness standard machine to be ± 0.1 HRC (± 2σ), and for standard test blocks a range of ± (0.1 – 0.2) HRC in seven indentations [25].

The effect of indenter shape has been widely investigated with different approaches to resolve the influence of cone radius and indenter angle on hardness variation [26 and 27]. Figures 11a and 11b summarise the various investigations

and shows the error in Rockwell HRC values caused by cone angle and spherical tip radius [28].

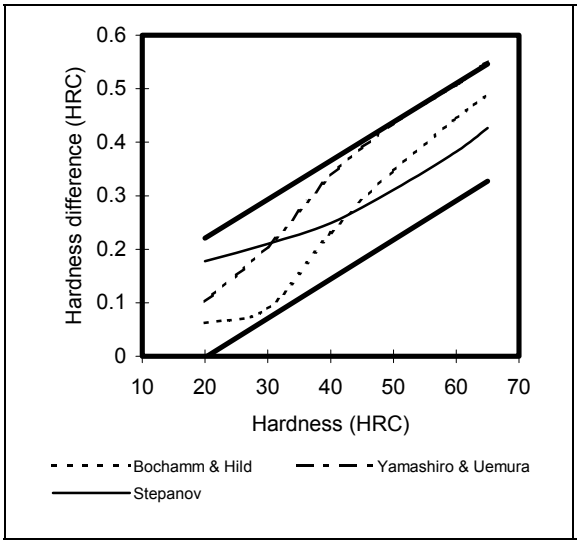

Figure 11a. Effect of a 0.01mm variation in indenter cone radius on the difference in measured hardness

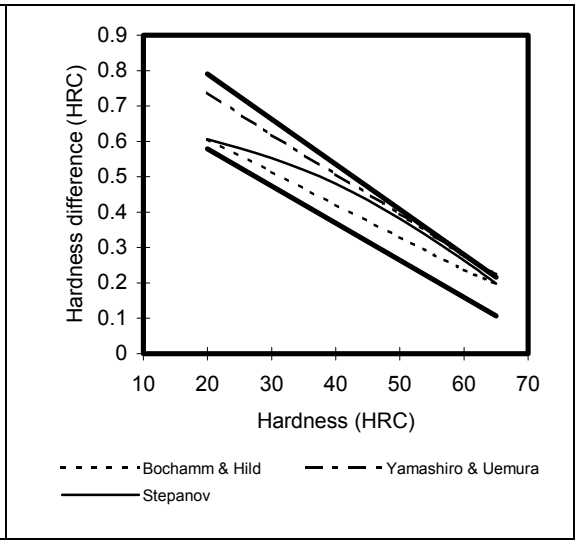

Figure 11b. Effect of a 30 minute variation in indenter cone angle on the difference in measured hardness

The envelope between the two continuous parallel lines contains the errors due to a radius difference of 0.01 mm and angular difference of 30 min, as reported by Petik [29]. Inside these envelopes are the lines corresponding to a theoretical evaluation of Bochmann and Hild [30] and Hild [31] and those proposed by Yamashiro and Uemura [32] and Stepanow [33]. These results are in general agreement with the practical experimentation carried out by Yamamoto and Yano [34] who reported that the uncertainty of hardness measurement contribution due to indenter shape was of the order of ± 1 HRC. However, this uncertainty contribution was lower than the experimental data reported by Wood et al [16]. This was because the experimental investigations did not determine second order effects of indenter geometry and that non-geometric factor could produce experimental noise to hide geometric effects. It should be noted that the contribution to uncertainty of the indenter, reported in these practical studies [34 and 16] are approximately a magnitude greater than that suggested by NIST (Table 4) for standard grade indenters, and demonstrates the need for further study.

IMGC have also investigated the contribution of Rockwell indenter shape in hardness measurement [28], and have carried out both experimental study and finite element analysis. The studies concentrated on gross geometric effects with cone angles ranging from approximately 118^{o} to 122^{o} and spherical tip radius from 180 μm to 220 μm. The investigation was carried out at three hardness levels: 25 HRC, 44 HRC, and 55 HRC. Table 5 shows the average of five hardness measurements. In general, these results show a similar trend to the HRC results observed by Wood et al [21].

Table 5. Hardness (H) and difference (ΔH) from quoted hardness value.

Indenter			Quoted hardness value 25.04 HRC		Quoted hardness value 44.20 HRC		Quoted hardness value 54.74 HRC	
	Tip radius (μm)	Cone angle (deg)	H (HRC)	ΔH (HRC)	H (HRC)	ΔH (HRC)	H (HRC)	ΔH (HRC)
1	175.5	118.62	22.68	-2.36	41.92	-2.28	52.64	-2.10
2	192.3	118.64	22.91	-2.13	42.27	-1.93	52.83	-1.91
3	227.7	118.33	23.54	-1.50	43.57	-0.63	54.69	-0.05
4	180.8	120.38	25.33	0.29	44.08	-0.12	54.37	-0.37
5	205.8	119.96	25.19	0.15	44.22	0.02	54.84	0.10
6	202.4	120.41	25.98	0.94	44.92	0.72	55.49	0.75
7	183.5	122.45	28.15	3.11	46.13	1.93	55.92	1.18
8	185.9	122.37	28.16	3.12	46.32	2.12	56.04	1.30
9	220.2	122.33	28.70	3.66	47.27	3.07	57.46	2.72

Table 6 compares the differences between the finite element analysis (FEA) and the experimental data. One advantage of the FEA model was that it allowed the individual contribution of indenter parameters on hardness measurement to be assessed.

Table 6. Difference between simulation and experimental data.

Indenter			Difference between simulation and experimental data (HRC)		
	Tip radius (μm)	Cone angle (deg)	Hardness value 25 HRC	Hardness value 44 HRC	Hardness value 55 HRC
1	175.5	118.62	-0.18	-0.06	-0.21
2	192.3	118.64	-0.16	-0.21	0.53
3	227.7	118.33	-0.19	0.26	0.47
4	180.8	120.38	-0.05	-0.42	-0.56
5	205.8	119.96	0.01	0.05	0.02
6	202.4	120.41	-0.07	-0.42	-0.62
7	183.5	122.45	0.18	-0.37	-0.57
8	185.9	122.37	0.15	-0.57	-0.63
9	220.2	122.33	0.26	-0.22	-0.43

Analysis of the results showed that, in general, the difference between the measured hardness and the FEA model increased with the test block hardness. Barbato et al [28] considered that these differences were due to three main sources of error: (i) the indenter shape, which was not as “ideal” as used in the model, (ii) the indenter roughness, which was dependent on machining differences; and (iii) the indenter hysteresis, which was controlled by production methodology. The FEA model, due to its idealisation and assumptions, also introduced errors; one assumption being that the coefficient of friction between the indenter and specimen was zero. Further analysis of the experimental results showed a linear correlation between differences in hardness with cone angle and radius at both 25 HRC and 44 HRC whilst, at 55 HRC, a second order effect was observed. Applying this

analysis to the FEA model showed second order effects at all hardness values. Further regression analysis showed that despite consideration of second order effects, no suitable experimental model could be proposed. The conclusion offered by Barbato et al [28] was that the experimental results were affected by factors associated with the micro-geometry (roughness) and/or deformation of the indenter under load, and recommended that these parameters required further investigation.

Despite the extensive research with Rockwell diamond indenters to establish the relationship between their geometry and performance, there are no clear conclusions. Other than that, it is not possible to predict the performance of an indenter from direct measurement of geometry. For this reason ISO standards [2] dictate that calibration indenters must be verified by comparison with reference standard grade indenters. Only the work at NIST [22, 23 and 24] has proposed any definition for standard indenters and their geometric characterisation. It is important, therefore, to develop a procedure to quantify the geometric characteristics of standard indenter for NMIs maintaining hardness standards. This importance has been recognised, and a CCM working group has proposed a work programme [35] that considers:

"*The indenter is a major source of the differences in Rockwell hardness measurements. An effort will be made to acquire a selection of National Metrological (standard grade) Rockwell diamond indenters. In order to accomplish this goal, it will be necessary to perform both geometric and performance comparisons of indenters.*

A future key comparison is planned for the systems used by NMIs for the geometrical measurement of Rockwell diamond indenters. The participating institutes will be IMGC, MPA, NIST, PTB and possibly NRLM and NPL"

The CCM will consider the influence of:

- cone angle,
- deviation from the straightness of the generatrix,
- spherical tip,
- inclination of the axis of the diamond cone to the axis of the indenter holder, and,
- roughness.

Recent work at NIST [36] investigating the performance of nine Rockwell diamond indenter has shown how tight control of tip radii, cone angles and form errors can significantly improve hardness measurement uncertainties. The study, investigated two manufacturers indenters that used a (110) and a (111) crystal axis orientation respectively. Measurement of the indenters showed that although the overall tip radius and cone angle were the same, the (110) orientated indenter exhibited a flat-shaped tip and four-lobed surface, whilst the (111) orientated indented displayed a sharp-shaped tip and a three-lobed surface. The mean tip radii of the nine indenters ranged from 197.25 μm to 202.43 μm, the mean cone angle ranged from 119.89° to 120.21°, and the cone flank straightness ranged from 0.15 μm to 0.49 μm. The hardness performances of the nine indenters are shown in Figure 12. The results show that for the mean hardness values of 25 HRC, 45 HRC and 63 HRC a total variation of – 0.23 to + 0.32 HRC. One of the indenters,

indicated by the arrow, possessed an increased surface roughness profile and this was suggested to be the reason for the performance bias.

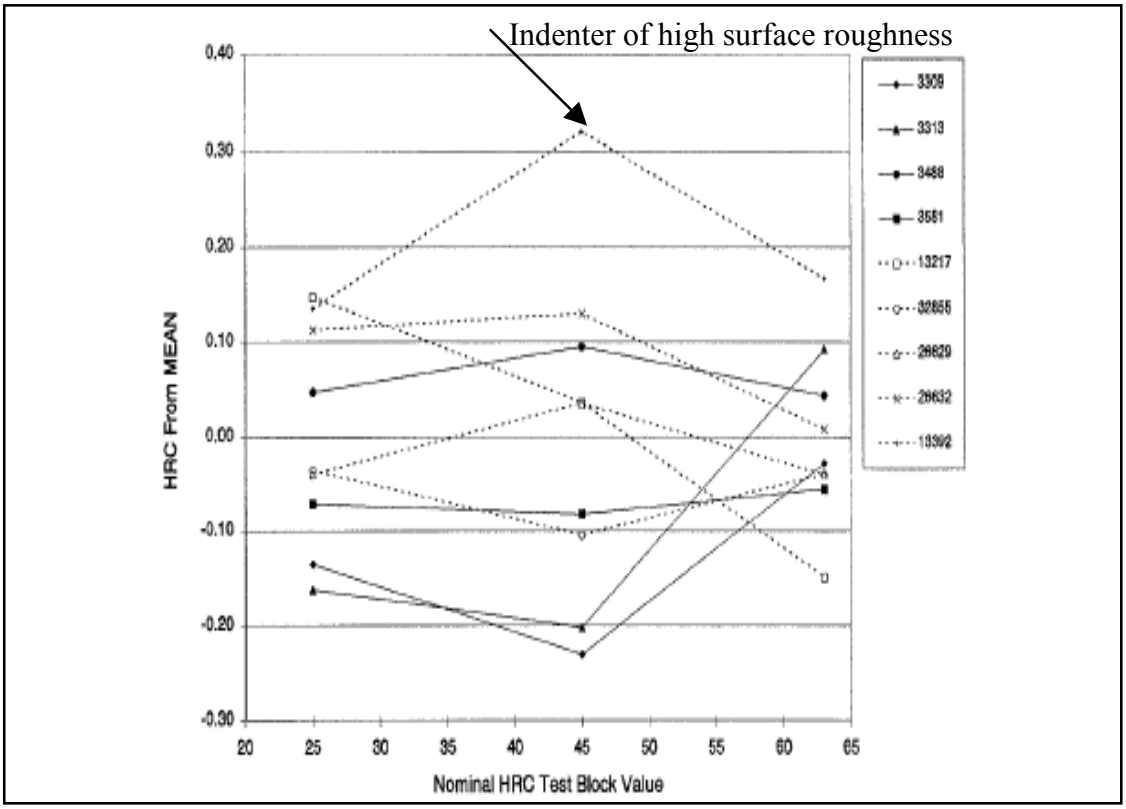

Figure 12. Performance comparisons of the nine indenters from the two manufacturers, the [110] indenters are the dotted lines and the [111] indenters are the solid lines.

From the literature, there is little evidence of any investigation into the influence of geometric characteristics of Brinell and Vickers indenters on performance, other than the recognition by PTB [36] that indenter morphology will contribute to the uncertainties of measurement. The most probable reason for this lack of research is that the uncertainty in the method of indentation measurement significantly out-weighs any contribution that the indenter may offer. An investigation by Yamamoto et al [13] showed the influence of indenter rigidity on hardness measurement. The results indicated only a minor influence in Vickers measurement whereas, considerable differences were observed with superficial Rockwell depth measurements. Yamamoto et al attributed these differences to the elastic deformation of the indenter, although the authors also considered creep and elastic recovery of the test blocks to provide a contribution, and that the homogeneity of the test block to have a greater contribution to the smaller indentation made by a superficial Rockwell indenter.

2.3 The Influence of the Indentation Measurement

The major uncertainty in determining Brinell and Vickers hardness is the measurement of the indentations and there is a need to consider the individual

contributions of the measurement chain, i.e. the optical system through to the final constituent, usually the human observer or computer image analysis systems.

Shin et al [38], in their investigation of Brinell indentation measurements, showed that lens magnification was a major contribution to the uncertainty budget. Analysis showed a difference between the ranges of lens magnification varying in around 3 HB, as shown in Figure 13. For example with the x 20 lens the indentation diameter was measured to be about 20 – 30 µm larger than the corresponding value with the x 100, a relative difference of the order 0.5 %.

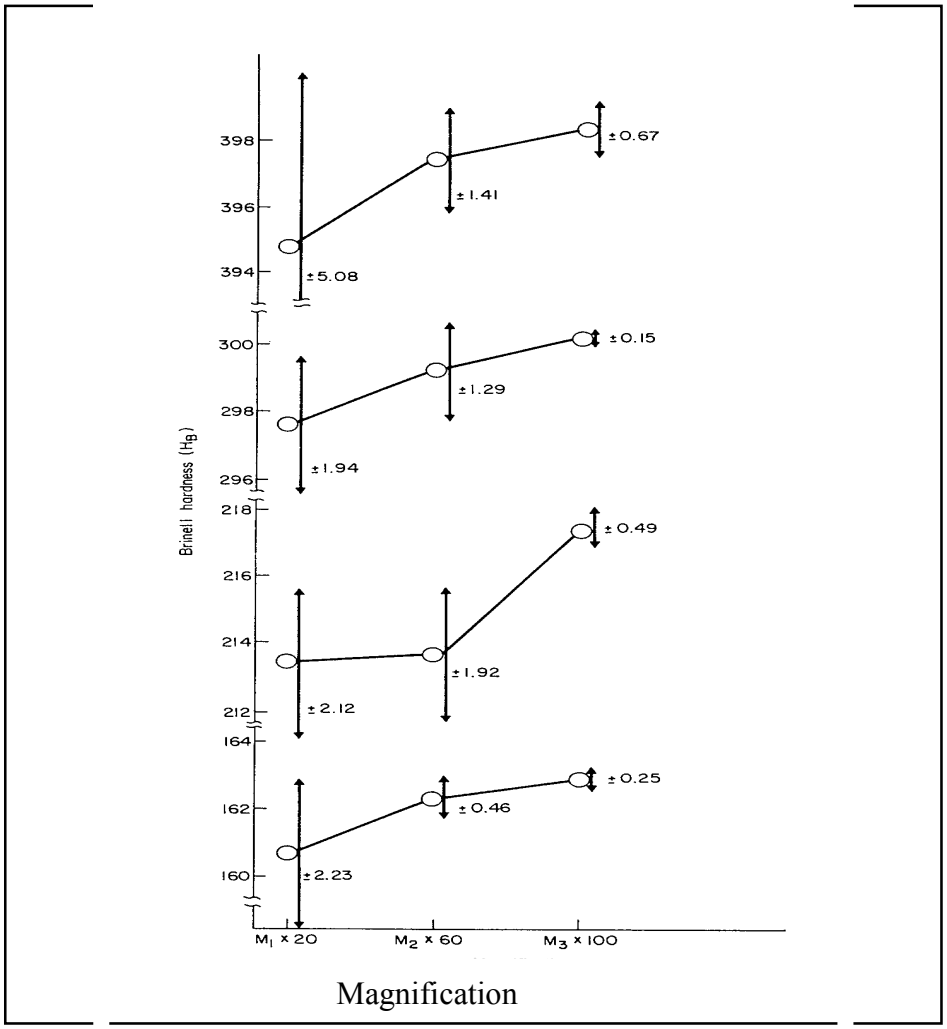

Figure 13. Difference in Brinell indentation measurements with different magnification objectives

Barbato and Desogus [41], have also analysed Shin et al's results and, in combination with their own investigations, conclude that the measurements of Brinell and Vickers indentations were the greatest contribution to the uncertainty in hardness, and the actual uncertainty was much higher than that specified in the Standards. They also concluded that it was important to describe the actual measurement methods applied in practice and attempt to quantify the possible source of measurement uncertainty. In Leigh's [40] investigation, he considered

the effect of the lens magnification on the diagonal measurements of a Vickers and Knoop indentation. Leigh's data is re-plotted (Figure 14), to show the variation in repeated measurements of a single indentation at different magnifications and numerical aperture (N.A).

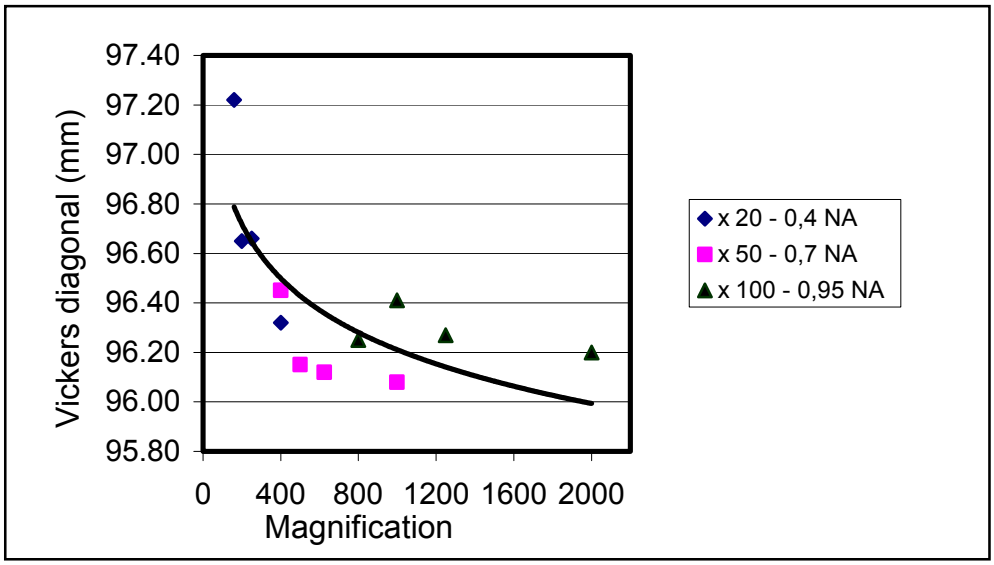

Figure 14. Average diagonal length of a single Vickers indentation at different magnifications.

Within the accuracy of these experiments, assuming a measurement uncertainty of a Vickers indentation of approximately 0.1 μm, Leigh concluded the following:

- At magnification greater than x 400, the measured indentation diagonal length does not appear to change.
- For objective lenses x 20 and x 50, the numerical aperture does not result in a difference in diagonal length.
- At x 20, however, the apparent diagonal length significantly increased with the reduction in overall magnification. This contradicts the theory, which states that for smaller NA the indentation length should be less than a high NA. The effect was also shown to be greater with soft blocks.
- Finally, the differences in measurement and the contradiction with theory were due to the 3-D nature of the indentation.

Tarasov and Thibault [41], and Thibault and Nyquist [42] have also investigated the effect of numerical aperture on the diagonal measurement of Knoop and Vickers indentation. Figure 15 shows the apparent differences in Vickers indentation measurement due to different numerical apertures. As it is impossible to separate the individual contributions of magnification and numerical aperture, no explanation was provided.

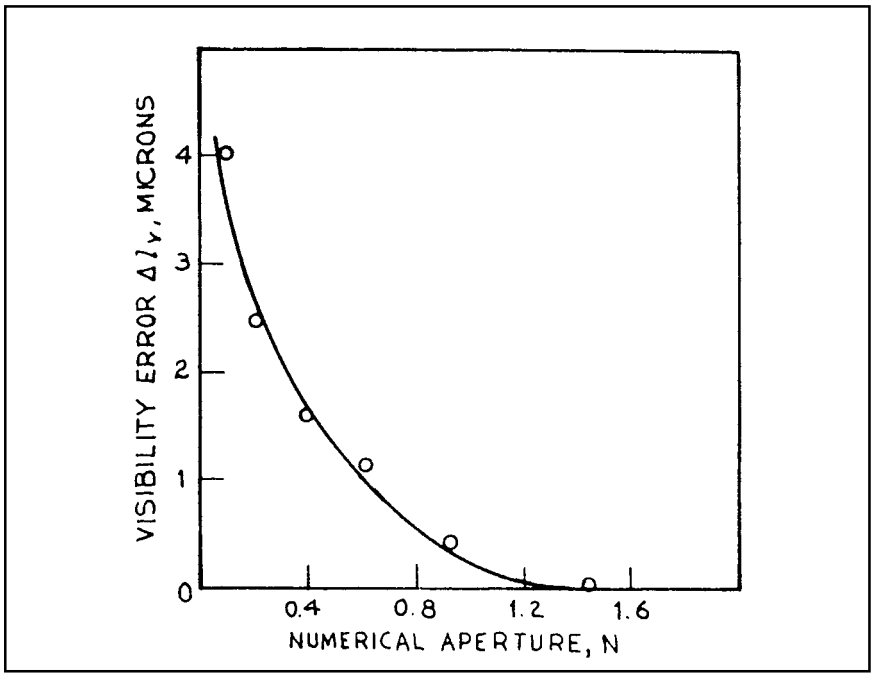

Figure 15. Differences in Vickers indentation measurement with different numerical aperture objective lenses.

Leigh's analysis of Figure 15 introduced correction factors that allow the generation of an empirical formula that indicated that the visibility error was proportional to 1 / (NA + 0.3), such that for an indentation measurement, using an objective of 0.95 NA, the uncertainty was 1.7 µm, increasing to 2.9 µm with a 0.40 NA objective. These figures were, however, specific to the microscope system used. Further, Leigh concluded that the error in measuring an indentation depended not only on the numerical aperture of the objective lens but also on the illumination conditions, and the ratio of the objective to condenser apertures.

Leigh also investigated the effect of changing the focal plane distance. The experiment examined an indentation of a Vickers diagonal length of approximately 70 µm, produced by a load of 2 kgf made in a test block of 800 HV nominal hardness. Once the position of best focus was determined, readings at 1 µm were made from between 5 µm below to 4 µm above this stage position. The experiment was repeated with the aperture stop varied to allow light through 99, 68, 38 and 10 % of the area of the objective area. Figure 16 shows a typical set of results.

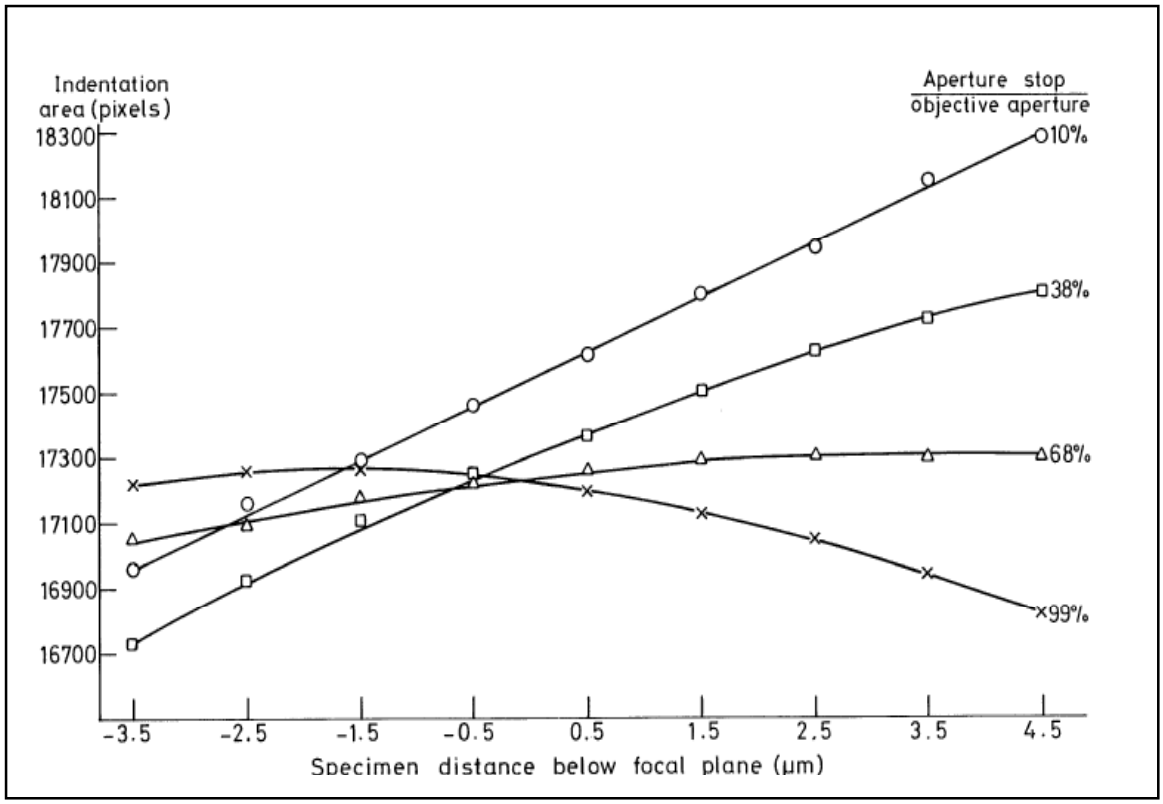

Figure 16. Apparent change in indentation area as a function of de-focus at various aperture stop positions

From these results it would appear that if the aperture was set to ~70 % the objective numerical aperture, then the indentation measurement would be the same regardless of the test block distance that the microscope is focused. If the percentage was greater, the apparent indentation size was reduced, and if smaller, the size increased. Focusing at any height above the surface gave erroneous results. The position at which the intersection occurred was considered the "true" focal plane. This was not necessarily the same position for the eyepiece and camera due to differences in focal distances. Focussing of the corners of the indentations was also important. This may not be the best focus for the entire indentation, due to "piling-up" or "sinking-in" of material along the sides. For this reason it is not advisable to use microscope auto-focusing devices in the measurement of indentations.

Barbato and Desogus [39] have investigated the effect of focal plane position and the changes caused by the numerical aperture in the measurement of Brinell indentations. Initial measurements were repeatedly made of a single indentation in a reference test block at the 200 HB 2.5/187.5 level. The major problem of the measurement was in the definition of the indentation diameter, particularly at low magnification. With the view of making the measurement easier a sharp notch close to the indentation was cut and the distance from its centre line to the apparent indentation boundary measured, under the various test conditions. Table 7 shows the displacements of this boundary line against an arbitrary zero point.

Table 7. Results from Barbato and Desogus experimental work [40]

Objective		Condition	Average image displacement (μm)	Standard. Dev of average (μm)
Magnification	NA			
5x	0.09	1	6.38	0.45
		2	5.55	0.45
10x	0.2	1	0.65	0.3
		2	1.18	0.15
10x	0.3	1	1.32	0.1
		2	0.81	0.15
20x	0.35	1	0.71	0.11
		2	0.53	0.09
20x	0.5	1	0.05	0.08
		2	0.2	0.08
50x	0.5	1	-0.03	0.08
		2	0	0.05

Condition 1 = normal position of focal plane
Condition 2 = focal plane distance increased by 40 mm

The results of Table 7 are shown graphically in Figure 17. Barbato and Desogus suggested that the measurements were dependent more on the numerical aperture of the lens than its focal plane.

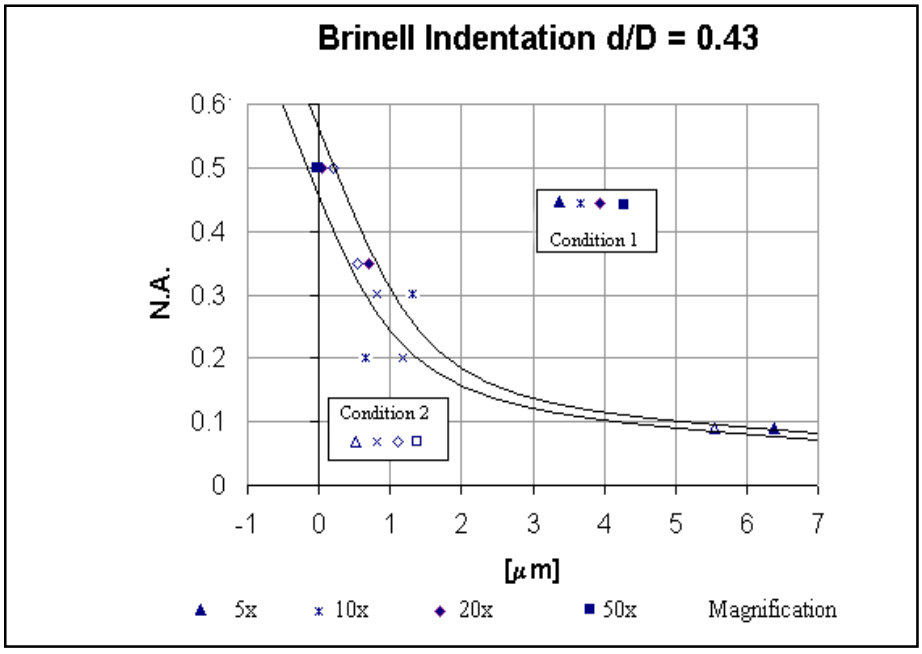

Figure 17. Trend of Brinell indentation measurements at two focal plane positions and different magnifications.

The effect of aperture on apparent indentation size has been investigated by Leigh [40]. Using a x 20, x 50 and x 100 objective lens with the x 1 intermediate condenser lens the diameter of the aperture stop was varied to ascertain any effect on the apparent size of Vickers indentations. Figure 18 show the apparent indentation size due to varying the size of the numerical aperture of the intermediate and objective lenses between 10 % and 100 %. Also included in this figure are results for the x 2 intermediate lens with the x 20 objective lens,

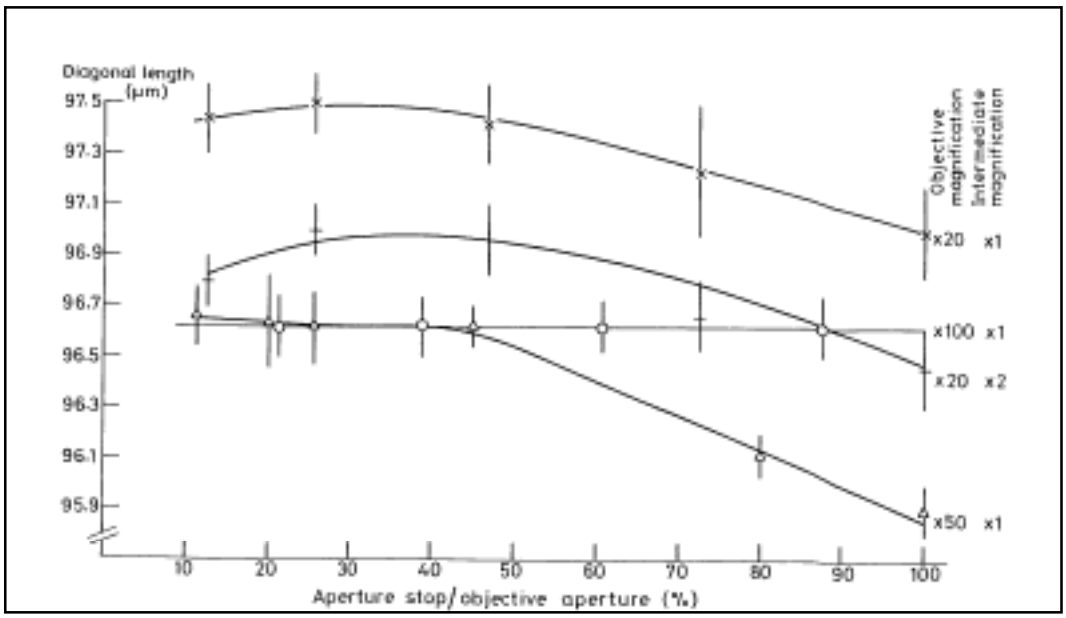

Figure 18. The effect of aperture stop position on apparent indentation depth.

The results showed that for the x 100 objective the NA of the condenser lens made no difference to the apparent indentation size whereas, for the x 50 and x 20 objectives a reduction in indentation measurement coinciding with a reduced aperture NA was observed. The effect of intermediate lens was to displace the curve, as shown for the x 20 objective. Leigh offered no conclusions to these observations.

In taking readings, with optical system, operators can make errors in the measured hardness value. Errors may vary between operators, the time of day or even the number of readings taken. The discrepancy in the values of different operators has been investigated by Hida and Yamatoto [43]. The investigation was carried out with three experienced operators measuring the same Vickers indentation, and then expanded to include three non-experienced operators. Individual operators showed differences of up to ± 2 μm, and a difference greater than 3 μm between the average values of roughly 50 measurements by different operators, as shown in Figure 19. A personal error for an experienced operators was estimated to be about 0.6 μm.

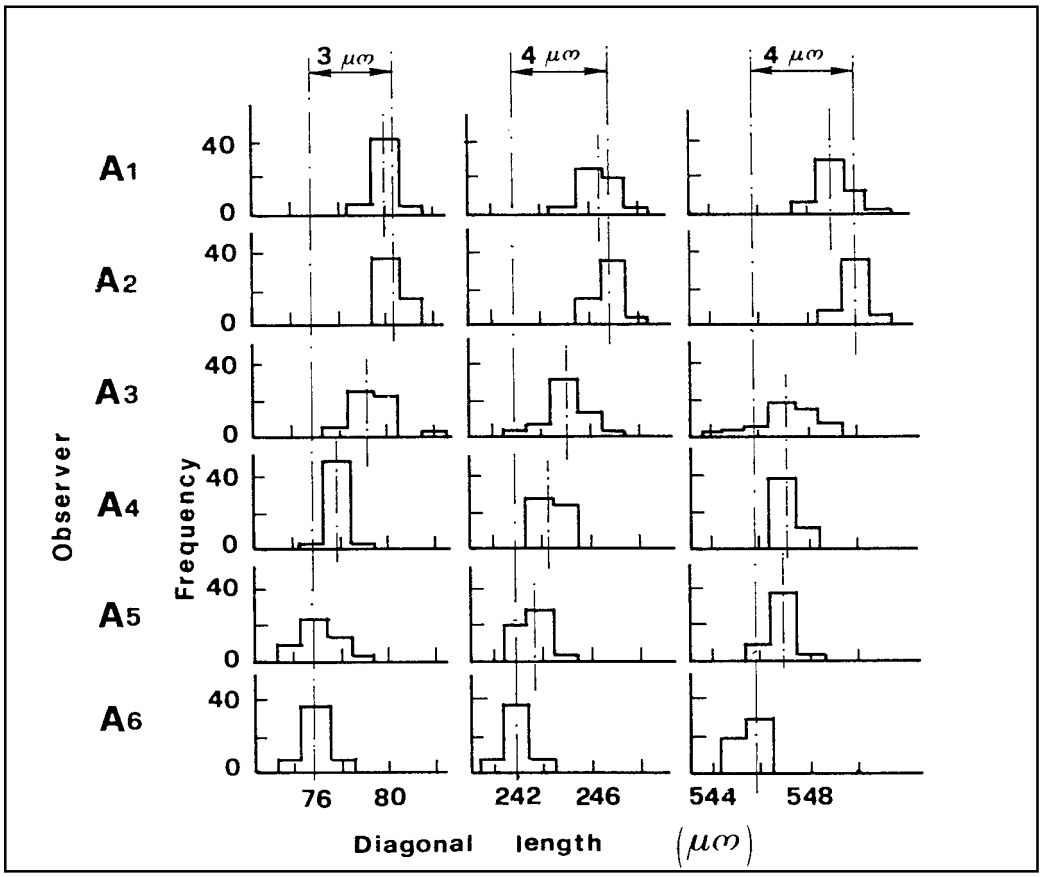

Figure 19. Distribution of Vickers indentation measurements by different operators

Indentations can also be measured using image analysis systems interfaced to a PC. There are two basic types: (i) direct measurement from one edge of an indentation to the other, or (ii) measurement of the either the area or volume of the indentation.

In Vickers hardness measurement, not only is the shape of the indention important but also measurement errors will be introduced if the edges of the indentation are incorrectly aligned. Although, this alignment is often dismissed as being only a cosine error, it is useful to know when the effect becomes significant. Figure 20 quantifies the error and shows that the rotation can be considerable before any significant error is introduced into the diagonal length.

θ	Cos θ	% Hardness error
1	0.9998	0.04
2	0.9994	0.12
3	0.9986	0.28
4	0.9976	0.48
5	0.9962	0.76
5.75	0.9950	1.0
8.10	0.9900	2.0

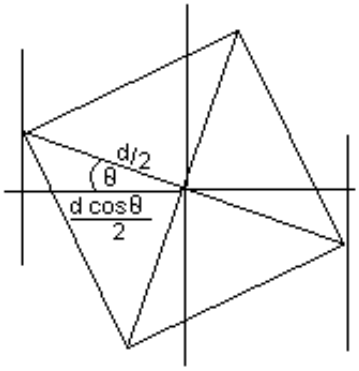

Figure 20. Error in hardness due to mis-orientation of the measured indentation [40]

Since the indentation area is required for a hardness calculation, the ideal situation would be direct measurement using image analysis. The area of indentation could then be calculated directly from the projected area divided by the cosine of the angle of inclination of the indentation to the surface. Unfortunately, with Vickers indentations, problems in measurement of the projected area occur due to a non-squareness of the indentation caused by either "piling-up" or "sinking-in" of material along the indentation sides. These departures from squareness will result in significant change in the projected area. In principle, it would be possible to make corrections, by measuring the perimeter of the indentation as well as its area. However, the measurement of such a small change in perimeter with sufficient accuracy to correct the area to an equivalent square would be very difficult [40] and considered impractical for Vickers indentations. Volume assessment can be made with greater accuracy when measuring Brinell indentations [44], and developed software to identify the location of the Brinell indentation has proved to be reliable and fast. Description of this measurement technique reports sensitivity due to both illumination and focus. A reduction in the illumination resulted in an apparent increase in the indentation diameter; similar observations were also made when the microscope stage was moved closer to the objective lens. These observations, in part, contradict with those of Leigh [40], who showed that as the stage was moved closer to the objective lens the apparent size of the indentation decreased.

The NPL image analysis system measures Brinell and Vickers hardness by either the diameter or the diagonal length of the indentations [45 and 46]. The software identifies the locations and measurement is by a combination of the movement of the microscope stage and screen position. The stage movement is measured by a Jamin interferometer with an uncertainty of less than 100 nm; calibration of the screen pixels is by the laser interferometer, or graticule. Angular alignment of Vickers indentations, as described in Figure 20, is accounted for. The system is fast, reliable and automated to eliminate operator error. At the time of writing the calibration of the image analysis system is under development to minimise the contribution to uncertainty. This development is based upon our understanding of image analysis variables as described in this report. One area that does require a

further understanding is the influence of microscope stage height position on the indentation size.

2.4 The Influence of the Test Block

In the performance-based hardness system, hardness scales are indirectly verified and disseminated to accredited hardness standards laboratories by the use of standard hardness test blocks. For the dissemination, the "true value" can only be measured if direct verification of the standard hardness machine has been previously carried out. The hardness values of the standard blocks also require being traceable to the individual manufacturing route, which should include conventional heat treatment processes of well-characterised ordinary industrial engineering materials. This characterisation must include the specification and verification of uniformity of the standard hardness test block's microstructure and its stability. A metallurgical study in Brazil [47] to enable home market production of Rockwell standard blocks has identified the role of microstructure homogeneity and conclude that oil quenching, to produce uniform cooling rates, was the best method to ensure uniform hardness. Machining of the test block should be carried out under closely controlled conditions to avoid any change to the surface physical and chemical properties of the material.

Figures 21a and 21b shows the results of an investigation of five sets of Rockwell hardness blocks carried out in China [48]. The result showed that the uniformity of each block was less than 0.19 HR, of which the majority (92 %) was less than 0.15 HR. These results were within the combined uncertainty of the hardness standard machine.

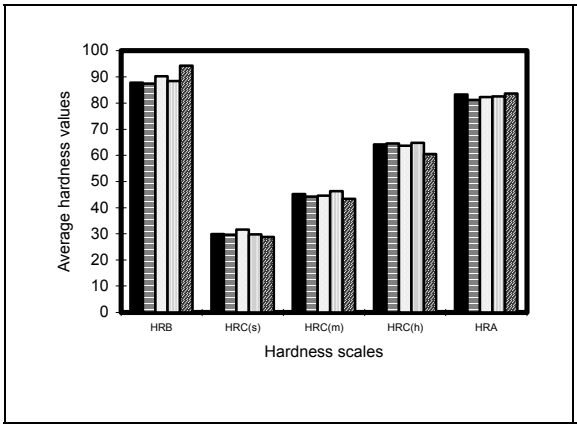

Figure 21a. Average Rockwell hardness of five test blocks

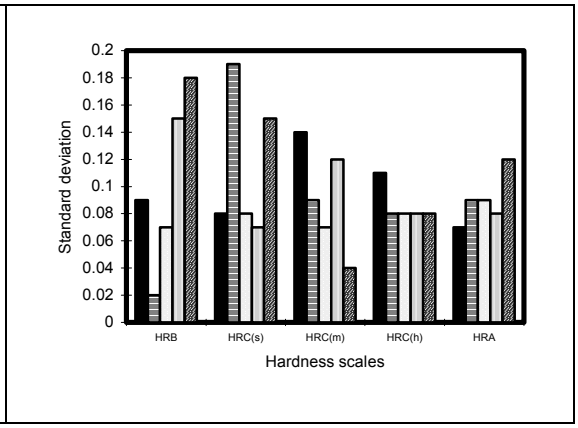

Figure 21b. Standard deviation of the hardness test blocks

Koike and Ishida [49] have also investigated the variability in Rockwell hardness standard test blocks and its contribution to uncertainty. Using the Japanese national standards hardness machine and making hardness measurement using the methodology shown in Figure 22, an average of nine values measured in nine zones, i.e. 81 measurements per block.

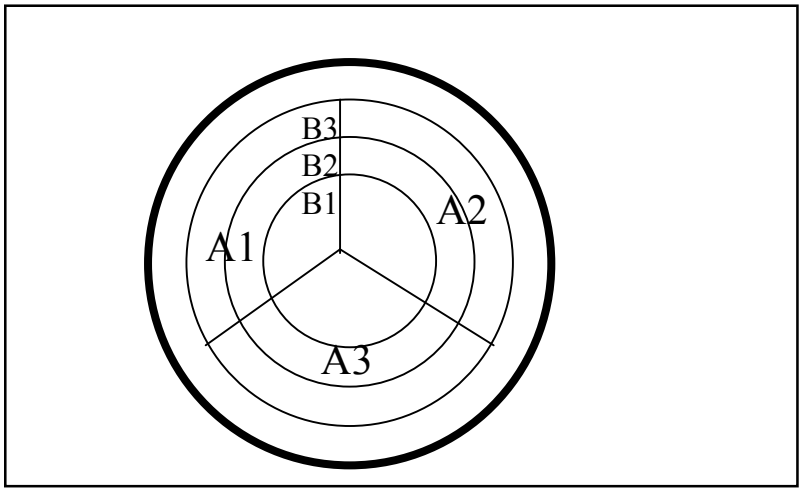

Figure 22. Hardness zones of Rockwell test block

In general, their results showed that for hard blocks, 60 HRC, differences in radial zones were observed, whereas for soft blocks, 20 HRC, differences in the circular zones were more significant. Further, the results showed that for a small area of the test block, typically a 10 mm diameter circle, the contribution to the standard uncertainty of the block was in the range 0.03 – 0.09 HRC, for the whole surface the contribution increased to a range of 0.06 – 0.18 HRC. Koike and Ishida also concluded that they were unable to forecast the distribution trend in any particular block and that the only way to provide a hardness distribution was to measure the whole surface of the test block, thus making it useless for further measurement.

In providing traceable hardness block, NIST have plotted how the hardness varied across the surface of a HRC hardness test block, and shown that it was possible to model this hardness variation [50]. This approach has resulted in two type of test block hardness certification: (i) the average hardness of the test block, and (ii) hardness at specific untested areas of the block. The second certificate providing a profile of how hardness varied across the surface and allowed the measurement uncertainty due to non-uniformity of the test block to be reduced. An example of a hardness profile across a Rockwell test block is shown in Figure 23.

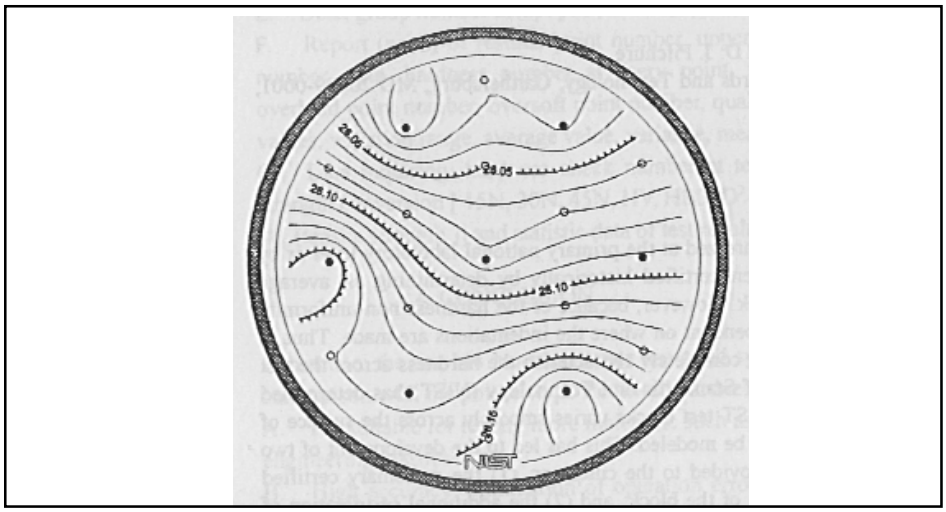

Figure 23. Hardness profile across the surface of NIST test block.

Seven hardness measurements were made at specific locations, as illustrated by the solid circles, the untested, modelled locations being illustrated by the open circles. The model to predict the hardness at the untested areas was based upon analysis of sample sets of reference test blocks to provide information on test block uniformity, or rather non-uniformity. For NIST reference test block the quoted measured hardness uniformity was within ± 0.2 HRC at the 25 HRC value, ± 0.15 HRC at the 45 HRC value, and ± 0.1 HRC at the $63 - 64$ HRC value. Hardness modelling provided improvement in the precision of hardness measurement by comparing the as-measured and modelled values, and calculation of more precise correction factors (Figure 24).

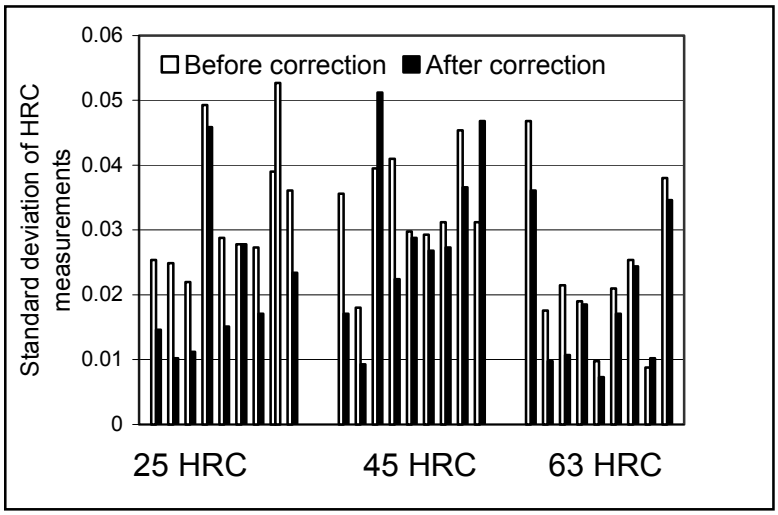

Figure 24. Standard deviation of HRC measurement, showing the effect of correction modelling on test block hardness.

Applying the more precise correction factors the standard deviation of hardness measurement were improved on average by 0.007, 0.005 and 0.003 for the 25, 45, and 63 - 64 HRC blocks respectively. However, this ability of NIST to model hardness variations across a Rockwell test block would appear to contradict the observations and conclusions of Koike and Ishida [49].

The contribution of standard test block cleanliness to the measured uncertainty of Brinell, Rockwell and Vickers measurement has been investigated at NPL [51], the instigation of the work was due to the increased usage of ultrasonic cleaning of standard test blocks prior to indentation. The results revealed that only the Brinell hardness measurement were influenced by the state of cleanliness, an increase of up to 3 % HB was recorded for cleaned blocks, whilst greasing the blocks gave a reduction in hardness of up to 1.6 %. The report provided little conclusive evidence on the influence of ultrasonic cleaning. However, the authors of this report consider that the increased cleanliness of the Brinell test block may provide improved definition of the indentation diameter, or that possibly the input of ultrasonic energy may work-harden the test block surface. The most probable influence of the grease is to reduce the indenter/test block friction to allow greater penetration.

2.5 Conclusions and Recommendations of Literature Review

This section has provided a review of the worldwide literature of the many factors contributing to uncertainty in hardness metrology, and highlights their complex interactions. The report systematically reviews the individual contributions of hardness machines, indenters, indentation measurement and test blocks to the measurement of hardness uncertainty, and finds contradiction in many of the reported results. Areas that require further research, include:

- Investigation of the Rockwell test cycle to investigate the importance of the specified rates of application of force and holding times on the measured hardness.
- Despite the immense amount of research on Rockwell diamond indenters, carried out primarily by NIST to establish a relationship between their morphology and performance, there are no clear conclusions. It is important to understand the influence of both geometric and non-geometric features of the Rockwell indenter on hardness measurement performance.
- Work is ongoing to understand the effect of microscope variables in the measurement of both Brinell and Vickers indentations such that repeatable results similar to those reported by IMGC can be achieved.

As mentioned, more work is required, into indenter effects, within the Vickers scale. The lack of work on their influence is possibly due to the uncertainty in the method of indentation measurement, but it has been identified that Vickers indenter morphology does contribute to the uncertainties in the hardness measurement. It would therefore be advisable to investigate these effects and also within the Rockwell scale, to compare results with those from other work.
For this reason the following work was carried out to try to identify these effects.

3. Indenter Characteristics Work

3.1 Protocol

The effect of the indenter morphology was identified as a main factor contributing to the hardness value (so work was done to determine the influence of the indenter characteristics.) The characteristics of both Rockwell and Vickers indenters were therefore investigated to identify the most important in order to concentrate specifically on those. (Based on the critical literature review and experience the characteristics of both Rockwell and Vickers indenters were identified.) Table 8 lists the characteristics and tolerances of Rockwell and Vickers indenters, as defined in the standard [2 and3].

Table 8. Characteristics of Vickers and Rockwell indenters.

Characteristics	
Rockwell	**Vickers**
Cone angle 120°±0.35°	**Angle 136±0.5°**
Flatness 0.002/0.4	Flatness
Off-axis angle ≤ 0.5°	Off-axis angle ≤ 0.5°
Tip radius 0.2 ± 0.01	Line of junction ≤ 0.002mm
	Base squareness

The properties in bold appeared, from the review, to be the most influential parameters on measured hardness, for their respective scale, have therefore been further investigated.

It was decided that indenters at the upper and lower limits of the accepted tolerances would be chosen to demonstrate the effect they could have on the overall hardness value while still remaining within the standard specifications.

Figure 25 shows the four indenters chosen for the Rockwell C scale, indicating which limits they meet.

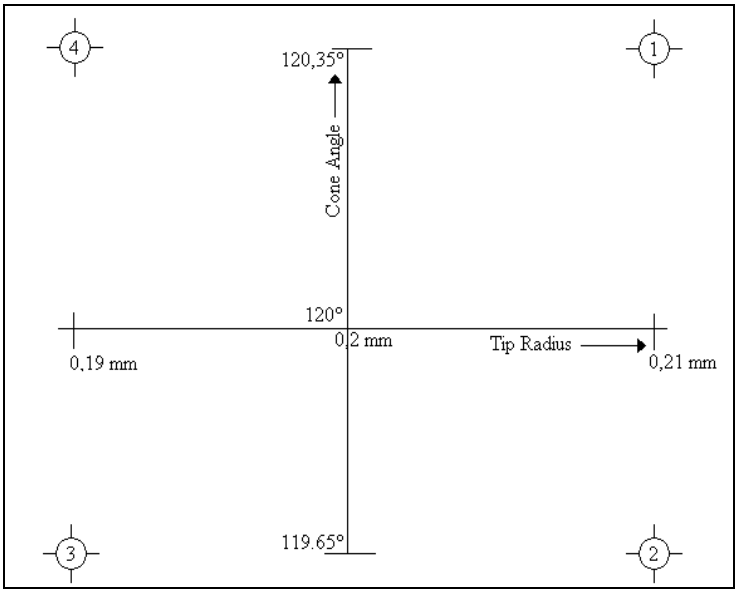

Figure 25 Rockwell indenter characteristics to be used:

Figure 26 shows the indenters chosen for the Vickers indenter characteristics work. Indenters of similar characteristics to 1,2 and 3, in the figure were purchased for this investigative work

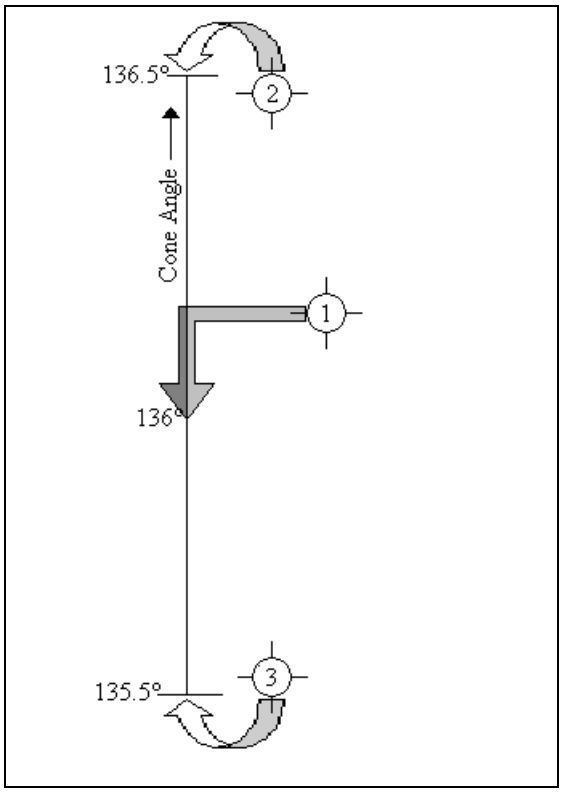

Figure 26 Vickers indenter characteristics to be used:

This indenter characteristics work was carried out across both HV10 and Rockwell C scales and across a range of hardnesses for both. NPL steel hardness reference blocks

were used for this work, each of which are standard Wilson hardness blocks of 60 mm diameter and 10 mm thickness. The test surface of the blocks is polished and marked with the NPL logo. For the HV10 scale, both HV10 800 and HV10 300 blocks were used. For the Rockwell C scale, both 63 HRC and 30 HRC blocks were used, as shown in Table 9.

Table 9. Indenters and blocks used

	Rockwell		**Vickers**	
	Hardness HRC	Serial No.	Hardness HV10	Serial No.
	30	TI0985	300	TI0985
	63	NII038	800	NII038
Indenters used with block: Serial No.	40222, 40223 40224, 40225		40226, 40227 40228	

The NPL hardness blocks are etched in the design shown in Figure 27. This etched map separates the block into five sections each consisting of either twelve or twenty-four spaces. Each section corresponds to one of the five areas and indentations are made by each of the indenters, spread across the block to allow for any inhomogeneity of the block. Figure 27 also shows the relevant locations for the indentations made by each indenter.

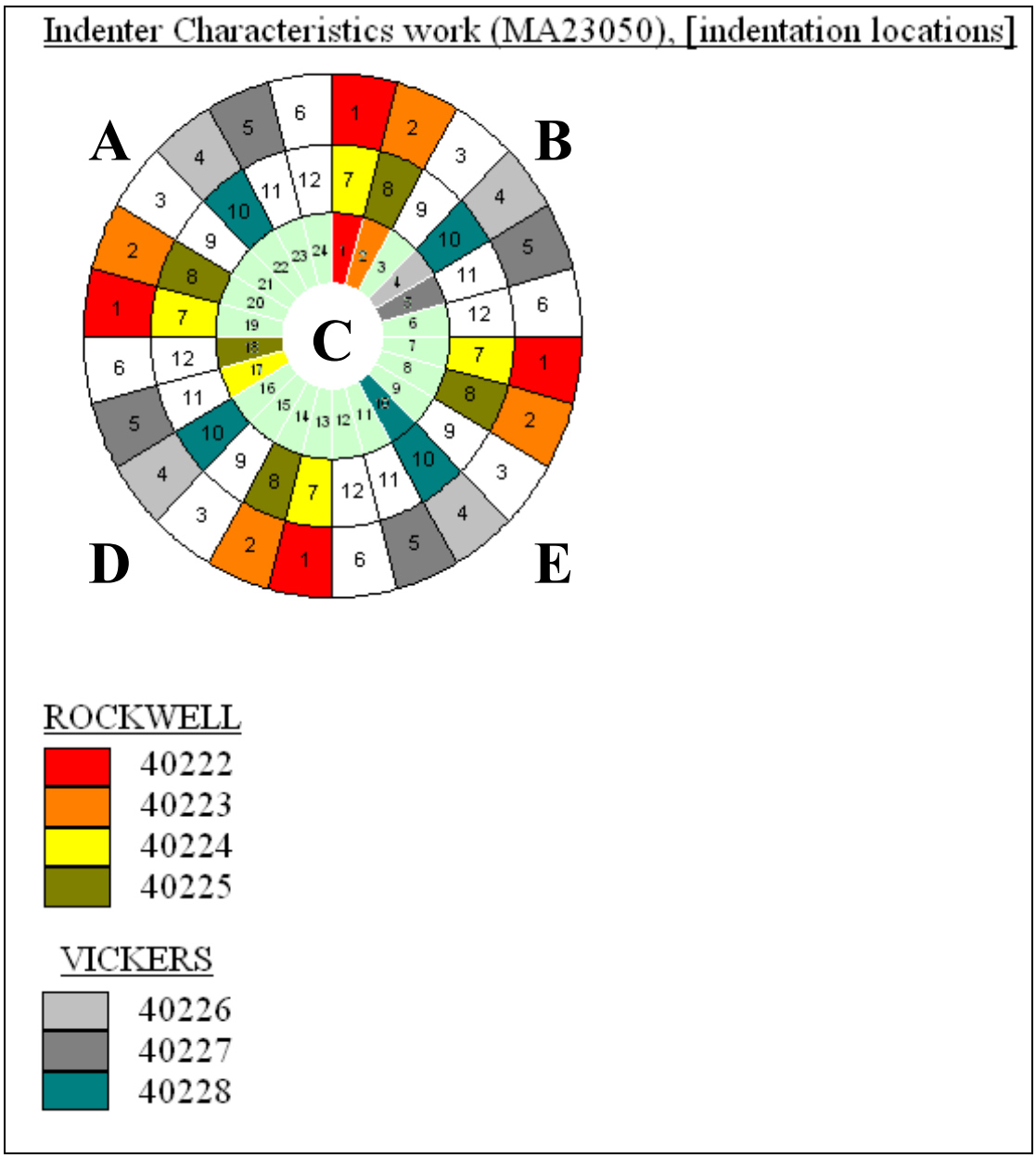

Figure 27 Indentation locations.

Five indentations were made with each indenter in the locations shown in Figure 27, using the NPL-Standard profiles for HRC and HV10 as shown in Table 10. For the HRC measurements, the control software was used to calculate the relevant hardness values for the block. This data was then stored in an Excel-compatible format for analysis. For the HV10 measurements the indentations were measured using NPL's indentation measuring kit.

Table 10. HRC and HV10 Profiles

Profile used within the Merlin software for HRC tests:

Ramp to Surface	up to 0.5 N at 0.1 mm/s
Ramp	up to 78.0 N at 0.01 mm/s
To Minor Load	up to 98.63 N for 2.0 s
Hold Load	3 s
To Major Load	up to 1478.6 N for 7.0 s
Hold Load	5 s
To minor Load	down to 98.71 N, for 5.0 s
Hold Load	5.0 s
Return	0.0 N

(The forces listed in the profile above and below are the values required to be input in the software to obtain the forces required by the standard, (98.07 N, and 1471 N), obtained via indirect calibration against the NPL force standard machines).

Profile used within the Merlin software for HV10 tests:

Ramp to Surface	up to 0.5 N at 0.1 mm/s
Ramp	up to 78.0 N at 0.01 mm/s
Ramp to Load	up to 98.63 N, for 3 s
Hold Load	13.0 s
Return	0.0 N

3.2 Work

3.2.1 Equipment

The work was carried out using NPL's 1.5 kN hardness machine (shown in Figure 28), which applies forces from 30 N to 1.5 kN.

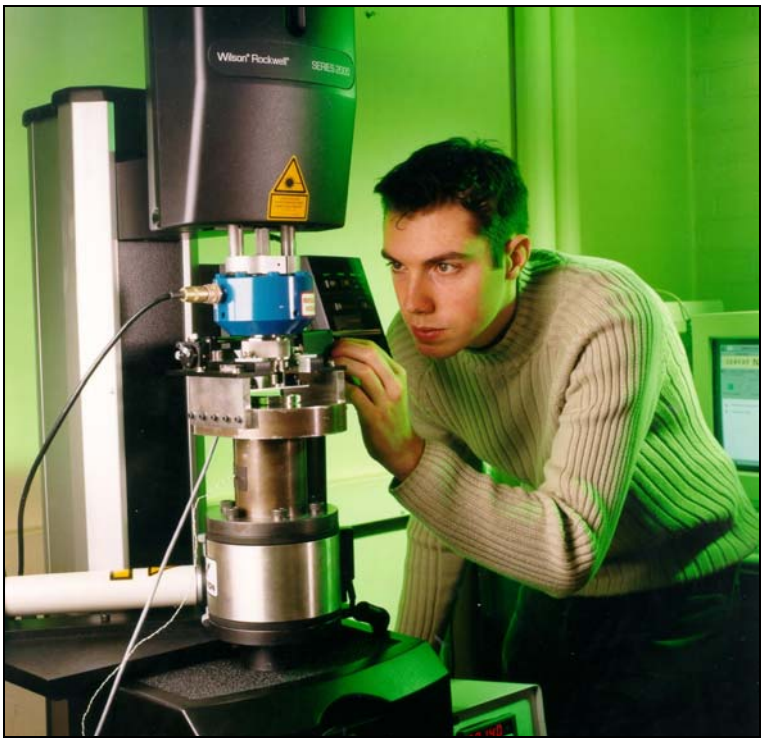

Figure 28. NPL 1.5 kN Hardness Machine.

The machine is designed with twin reaction columns to eliminate torque from the screw drive. High accuracy load cells, traceable to NPL force standard machines, measure the applied force. Indenter depth measurement is by a laser interferometer system, the indenter is located centrally within the holder, which measures from the mounted lenses on either side of the indenter tip (Figure 29). This interferometer is traceable to the UK realisation of metre at NPL. Time control of the loading cycle and measurement of the indenter velocity is calibrated against the UK time standard at NPL.

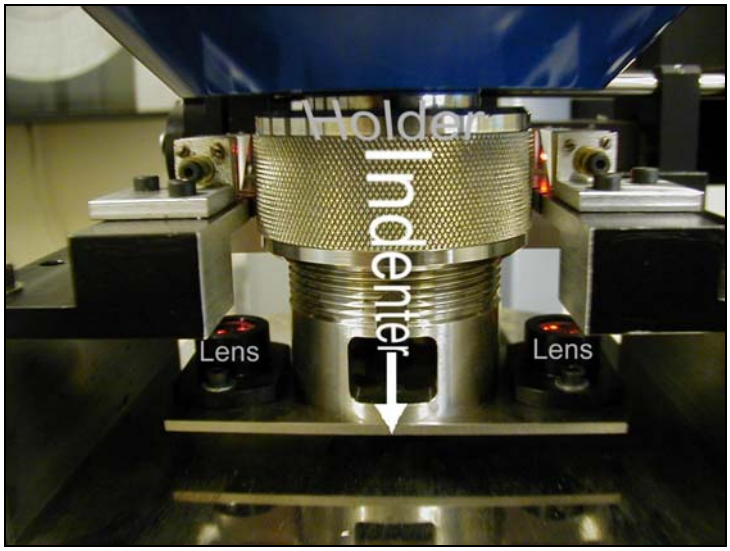

Figure 29. Close-up of hardness machine depth measuring system.

The 1.5kN hardness machine is based on the Instron RT2000 hardness machine, and is able to cover demands of the Rockwell scales HRA-HRK and superficial Rockwell scales from HR15N to HR45T [45]. In addition, the machine is able to meet the forces requirements of Vickers scales from HV5 to HV100 and the Brinell scales from HB2/4 to HB5/125. The machine is interfaced to its own PC-driven control system based upon Instron's Merlin and Wavemaker software product. This software uses generalised waveforms for closed loop control. The servo design provides control of the applied force and indenter motion and avoids the risk of load overshoot present in some deadweight machines.

The uncertainty in the hardness measurement with this machine for Rockwell is ±0.2 % (at a 95 % level of confidence), and ±0.3 % (at a 95 % level of confidence) for Vickers.

The Vickers indentations are measured using a microscope with CCD camera to image the indentation, an interferometer to measure the movement of the stage, and image analysis software that controls the measurement process Figure 30. The software system has been developed by Graftek Italia Srl for IMGC. This system minimises human manipulation of "cross hairs" in identifying the diagonal vertexes of a Vickers indentation in an automated process.

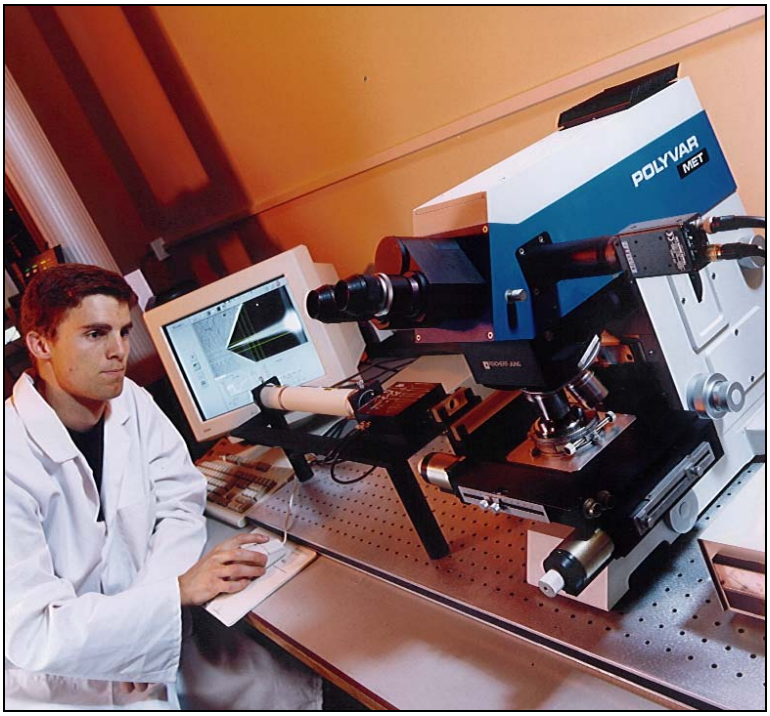

Figure 30. Indentation measuring system.

Figure 31 shows the indenter characterisation system, developed by LTF Gal-Indent for IMGC. The system contains: (i) an interferometer sine bar, for angle/geometry of Vickers indenters and cone/tilt angles of Rockwell indenters, and (ii) a rotary table for measuring the spherical tip of Rockwell indenters.

Figure 31. LTF Gal-Indent system.

The sine bar workstation is based on Mirau interferometer mounted on a metallurgical microscope equipped with a x10 DI objective lens. To evaluate the angle of the faces of a Vickers indenter, an indenter is placed in the sine bar and tilted until a diffraction pattern is observed on one of its faces. The number of fringes is minimised to ensure that the face of the indenter is perpendicular to the lens.

When the face is perpendicular to the lens the movement of the sine bar is measured and used to calculate the angle of the indenter face relative to the shaft. The angle of the cone of a Rockwell indenter is evaluated using a similar technique. The flatness of each face can be determined from the number of fringes seen when the face is aligned perpendicular to the lens and the offset line determined from on screen measurement using a 100x lens.
The rotary table uses an LVDT to measure the radius of the tip of a Rockwell indenter. The table rotates around the tip of the indenter to measure any deviation of the radius of the tip from the ideal value of 200 μm.
Both systems are connected to a computer system that performs automatic data acquisition.
All the indenters used were characterised before use using the NPL system.

3.2.2 Vickers HV10

Indenter Characterisation:
Table 11, details the characteristics, as measured using the NPL Gal-indent system, (Figure 31), of each of the three Vickers indenters used.

Table 11. Indenters SN. 40226, 40227 and 40228 Characterisation.

NPL Characterisation:

Vickers Indenter Serial No: 40226
Average Angle = 135.616 Std Dev = 0.019
Tilt Angle = 0.060 Std Dev = 0.005

Vickers Indenter Serial No: 40227
Average Angle = 136.143 Std Dev = 0.008
Tilt Angle = 0.045 Std Dev = 0.008

Vickers Indenter Serial No: 40228
Average Angle = 136.639 Std Dev = 0.009
Tilt Angle = 0.033 Std Dev = 0.002

Tables 12 and 13 show the measured diagonals of all the Vickers indentations made on both blocks. They also include the temperature range for each measurement session and the lens combination used. All the measurements were made using the NPL Indentation measuring system (Figure 30).

Table 12. 300 HV10 measurement results

300 HV10 Block

	Main	Secondary
Lenses	x20	x0.8
Temp:	20.4°- 20.9°	
Indenter	**Block**	
40226	**TI0985**	
Indent	Mean diagonal (μm)	
1	240.755	
2	241.133	
3	241.223	
4	241.453	
5	240.905	
Overall mean	241.094	

	Main	Secondary
Lenses	x20	x0.8
Temp:	20.4° - 20.8°	
Indenter	**Block**	
40227	**TI0985**	
Indent	Mean diagonal (μm)	
1	240.897	
2	241.415	
3	242.118	
4	240.633	
5	241.137	
Overall mean	241.240	

	Main	Secondary
Lenses	x20	x0.8
Temp:	20.5° - 20.9°	
Indenter	**Block**	
40228	**TI0985**	
Indent	Mean diagonal (μm)	
1	243.462	
2	242.008	
3	242.642	
4	241.592	
5	243.558	
Overall mean	242.652	

Table 13. 800 HV10 measurement results

800 HV10 Block

	Main	Secondary
Lenses	x20	x1.25
Temp	20.5° - 20.9°	
Indenter	**Block**	
40226	**NI1038**	
Indent	Mean diagonal (μm)	
1	149.858	
2	149.963	
3	150.430	
4	150.210	
5	149.792	
Overall mean	150.051	

	Main	Secondary
Lenses	x20	x1.25
Temp	20.4° - 20.7°	
Indenter	**Block**	
40227	**NI1038**	
Indent	Mean diagonal (μm)	
1	150.035	
2	150.173	
3	150.395	
4	150.428	
5	150.092	
Overall mean	150.225	

	Main	Secondary
Lenses	x20	x1.25
Temp	20.4° - 20.7°	
Indenter	**Block**	
40228	**NI1038**	
Indent	Mean diagonal (μm)	
1	150.657	
2	150.253	
3	150.380	
4	150.643	
5	150.870	
Overall mean	150.561	

Tables 14 and 15 are the combined results of tables 12 and 13. They display all the mean indentation diameters and their conversion to the HV10 hardness value.

Table 14. 300 HV10 calculated hardnesses

	300HV10		
	40226	**40227**	**40228**
	d/μm	d/μm	d/μm
1	240.755	240.897	243.462
2	241.133	241.415	242.008
3	241.223	242.118	242.642
4	241.453	240.633	241.592
5	240.905	241.137	243.558
Average:	241.094	241.24	242.652
	HV	**HV**	**HV**
1	320.023	319.647	312.947
2	319.020	318.276	316.717
3	318.782	316.429	315.066
4	318.175	320.347	317.811
5	319.625	319.011	312.699
Average:	**319.125**	**318.742**	**315.048**
* .	**318.690**	**318.898**	**315.743**

* Hardness based on using exact indenter geometry in equation

Table 15. 800 HV10 calculated hardnesses

	800HV10		
Indenter:	**40226**	**40227**	**40228**
	d/μm	d/μm	d/μm
1	149.858	150.035	150.657
2	149.963	150.173	150.253
3	150.430	150.395	150.380
4	150.210	150.428	150.643
5	149.792	150.092	150.870
Average	150.051	150.225	150.561
Hardness	**HV**	**HV**	**HV**
1	825.982	824.038	817.251
2	824.825	822.520	821.645
3	819.716	820.097	820.261
4	822.119	819.734	817.396
5	826.717	823.416	814.941
Average	**823.872**	**821.961**	**818.299**
*	**822.745**	**822.372**	**820.124**

* Hardness based on using exact indenter geometry in equation

3.2.3 Rockwell C

Table 16 shows the resulting average angle and tilt angle calculated from characterisation of the Rockwell indenters, as measured using the NPL Gal-indent system, (Figure 31).

Indenter Characterisation:

Table 16. Rockwell indenters, SN 40222, 40223, 40224 and 40225 Characterisation

NPL Characterisation:		
Rockwell Indenter Serial No: 40222		
		Std Dev
Av Angle	= 120.244	0.016
Tilt Angle	= 0.034	0.012
Tip Radius = 0.1915 mm		
Rockwell Indenter Serial No: 40223		
		Std Dev
Av Angle	= 120.286	0.033
Tilt Angle	= 0.060	0.007
Tip Radius	= 0.209 mm	
Rockwell Indenter Serial No: 40224		
		Std Dev
Av Angle	= 119.566	0.016
Tilt Angle	= 0.059	0.010
Tip Radius = 0.189 mm		
Rockwell Indenter Serial No: 40225		
		Std Dev
Av Angle	= 119.569	0.022
Tilt Angle	= 0.052	0.010
Radius	= 0.210 mm	

Tables 17 to 26 show the results obtained from the Rockwell measurements using the 1.5 kN hardness machine, with all four indenters on both hardness blocks. Tables 21 and 26 compile the hardness readings for each block and each indenter for later analysis.

Table 17. 30 HRC measurement results for indenter 40222

30 HRC Indenter: 40222	**Initial Depth (mm)**	**Final Depth mm**	**Depth (mm)**	**Hardness Value [HRC]**
1	0.50449	0.64011	0.13562	32.19
2	0.5106	0.64608	0.13547	32.26
3	0.51013	0.64526	0.13513	32.43
4	0.50561	0.64167	0.13606	31.97
5	0.51621	0.65091	0.1347	32.65
Mean	**0.50941**	**0.6448**	**0.1354**	**32.30**
Standard Deviation	0.00466	0.00421	0.00051	0.26
Coefficient of Variation	0.91513	0.65355	0.37952	0.80
Median	0.51013	0.64526	0.13547	32.26
Mean + Standard Deviation	0.51407	0.64902	0.13591	32.56
Mean - Standard Deviation	0.50475	0.64059	0.13488	32.05
Minimum	0.50449	0.64011	0.1347	31.97
Maximum	0.51621	0.65091	0.13606	32.65

Table 18. 30 HRC measurement results for indenter 40223

30 HRC Indenter: 40223	**Initial Depth (mm)**	**Final Depth mm**	**Depth (mm)**	**Hardness Value [HRC]**
1	1.02435	1.15807	0.13371	33.14
2	1.02249	1.15616	0.13366	33.17
3	1.0223	1.15661	0.13431	32.84
4	1.03092	1.15443	0.13352	33.24
5	1.02819	1.1617	0.1335	33.25
Mean	**1.02565**	**1.15939**	**0.13374**	**33.13**
Standard Deviation	0.00378	0.00356	0.00033	0.17
Coefficient of Variation	0.36842	0.30714	0.2478	0.50
Median	1.02435	1.15807	0.13366	33.17
Mean + Standard Deviation	1.02943	1.16295	0.13407	33.30
Mean - Standard Deviation	1.02187	1.15583	0.13341	32.96
Minimum	1.0223	1.15616	0.1335	32.84
Maximum	1.03092	1.16443	0.13431	33.25

Table 19. 30 HRC measurement results for indenter 40224

30 HRC Indenter: 40224	Initial Depth (mm)	Final Depth mm	Depth (mm)	Hardness Value [HRC]
1	1.07462	1.21418	0.13957	30.22
2	1.07509	1.21312	0.13803	30.98
3	1.07873	1.21698	1.3825	30.87
4	1.08293	1.22034	1.3741	31.29
5	1.07964	1.21727	1.3763	31.18
Mean	**1.0782**	**1.21638**	**1.3818**	**30.91**
Standard Deviation	0.00344	0.00284	0.00084	0.42
Coefficient of Variation	0.31871	0.23363	0.60938	1.36
Median	1.07873	1.21698	0.13803	30.98
Mean + Standard Deviation	1.08164	1.21922	0.13902	31.33
Mean - Standard Deviation	1.07476	1.21354	0.13734	30.49
Minimum	1.07462	1.21312	0.13741	30.22
Maximum	1.08293	1.22034	0.13957	31.29

Table 20. 30 HRC measurement results for Indenter 40225

30 HRC Indenter: 40225	Initial Depth (mm)	Final Depth mm	Depth (mm)	Hardness Value [HRC]
1	0.67231	0.81039	0.13807	30.96
2	0.67442	0.81221	0.13779	31.11
3	0.67608	0.81395	0.13787	31.06
4	0.6801	0.81742	0.13732	31.34
5	0.67911	0.81646	0.13735	31.33
Mean	**0.6764**	**0.81408**	**0.13768**	**31.16**
Standard Deviation	0.00323	0.00291	0.00033	0.17
Coefficient of Variation	0.47773	0.35799	0.24182	0.53
Median	0.67608	0.81395	0.13779	31.11
Mean + Standard Deviation	0.67964	0.817	0.13801	31.33
Mean - Standard Deviation	0.67317	0.81117	0.13735	30.99
Minimum	0.67231	0.81039	0.13732	30.96
Maximum	0.6801	0.81742	0.13807	31.34

Table 21. Compiled results of HRC Indenters on 30 HRC block

30 HRC	Hardness Value [HRC]			
Indenter:	**40222**	**40223**	**40224**	**40225**
1	32.19	33.14	30.22	30.96
2	32.26	33.17	30.98	31.11
3	32.43	32.84	30.87	31.06
4	31.97	33.24	31.29	31.34
5	32.65	33.25	31.18	31.33
Mean	**32.3**	**33.13**	**30.91**	**31.16**

Table 22. 63 HRC measurement results for Indenter 40222

63 HRC Indenter: 40222	Initial Depth (mm)	Final Depth mm	Depth (mm)	Hardness Value [HRC]
1	0.45841	0.53011	0.0717	64.15
2	0.46159	0.53331	0.07172	64.14
3	0.45993	0.53224	0.07231	63.84
4	0.46057	0.53216	0.07159	64.21
5	0.46464	0.53635	0.07171	64.15
Mean	**0.46103**	**0.53683**	**0.07181**	**64.1**
Standard Deviation	0.00232	0.00228	0.00029	0.14
Coefficient of Variation	0.50406	0.42761	0.40124	0.22
Median	0.46057	0.53224	0.07171	64.15
Mean + Standard Deviation	0.46335	0.53511	0.07209	64.24
Mean - Standard Deviation	0.4587	0.53056	0.07152	63.95
Minimum	0.45841	0.53011	0.07159	63.84
Maximum	0.46464	0.53635	0.07231	64.21

Table 23. 63 HRC measurement results for Indenter 40223

63 HRC Indenter: 40223	Initial Depth (mm)	Final Depth mm	Depth (mm)	Hardness Value [HRC]
1	0.97162	1.04147	0.06985	65.07
2	0.97536	1.04485	0.06949	65.26
3	0.97299	1.04297	0.06998	65.01
4	0.97276	1.04228	0.6952	65.24
5	0.97694	1.0465	0.06956	65.22
Mean	**0.97393**	**1.04362**	**0.06968**	**65.16**
Standard Deviation	0.00216	0.00204	0.00022	0.11
Coefficient of Variation	0.22198	0.19547	0.31557	0.17
Median	0.97299	1.04297	0.06956	65.22
Mean + Standard Deviation	0.9761	1.04566	0.0699	65.27
Mean - Standard Deviation	0.97177	1.04158	0.06946	65.05
Minimum	0.97162	1.04147	0.06949	65.01
Maximum	0.97694	1.0465	0.06998	65.26

Table 24. 63 HRC measurement results for Indenter 40224

63 HRC Indenter: 40224	Initial Depth (mm)	Final Depth mm	Depth (mm)	Hardness Value [HRC]
1	1.02494	1.0995	0.07456	62.72
2	1.02844	1.10204	0.0736	63.2
3	1.02641	1.10037	0.07396	63.02
4	1.02737	1.10085	0.07348	63.26
5	1.03041	1.10373	0.07332	63.34
Mean	**1.02752**	**1.1013**	**0.07378**	**63.11**
Standard Deviation	0.00207	0.00164	0.00049	0.25
Coefficient of Variation	0.20124	0.14896	0.66902	0.39
Median	1.02737	1.10085	0.0736	63.2
Mean + Standard Deviation	1.02958	1.10294	0.07428	63.36
Mean - Standard Deviation	1.02545	1.09966	0.07329	62.86
Minimum	1.02494	1.0995	0.07332	62.72
Maximum	1.03041	1.10373	0.07456	63.34

Table 25. 63 HRC measurement results for Indenter 40225

63 HRC Indenter: 40225	Initial Depth (mm)	Final Depth mm	Depth (mm)	Hardness Value [HRC]
1	0.62535	0.69808	0.07274	63.63
2	0.62818	0.70048	0.0723	63.85
3	0.6255	0.69829	0.07279	63.6
4	0.62641	0.69852	0.07211	63.95
5	0.62953	0.70183	0.0723	63.85
Mean	**0.62699**	**0.69944**	**0.07245**	**63.78**
Standard Deviation	0.00181	0.00164	0.0003	0.15
Coefficient of Variation	0.28862	0.23463	0.4152	0.24
Median	0.62641	0.69852	0.0723	63.85
Mean + Standard Deviation	0.6288	0.70108	0.07275	63.93
Mean - Standard Deviation	0.62518	0.6978	0.07215	63.63
Minimum	0.62535	0.69808	0.07211	63.6
Maximum	0.62953	0.70183	0.07279	63.95

Table 26. Compiled results of HRC Indenters on 63 HRC block

63 HRC	Hardness Value [HRC]			
Indenter:	**40222**	**40223**	**40224**	**40225**
1	64.15	65.07	62.72	63.63
2	64.14	65.26	63.2	63.85
3	63.84	65.01	63.02	63.6
4	64.21	65.24	63.26	63.95
5	64.15	65.22	63.34	63.85
Mean	**64.1**	**65.16**	**63.11**	**63.78**

3.3 Analysis

3.3.1 Vickers

To understand more about the possible reasons that the indenters give different measured hardnesses we need to compare their different measured properties. Figure 32, gives the results obtained from the three Vickers indenters used with 300 HV10 block. Indenter 40228 produces a lower hardness value than 40227, which is similar to but slightly lower than 40226.

Figure 32 also gives the mean hardness value obtained for the HV10 300 block by each of the indenters. This value has then been plotted against the varying indenter angle of each indenter. There appears to be a definite trend, with the measured block hardness decreasing with the increase in the Vickers indenter angle, to an amount of approx 4 HV from the lower to the upper boundary of the standard for Vickers indenters. The trend is still visible, although less distinct between indenter angles of 135.5° and 136°.

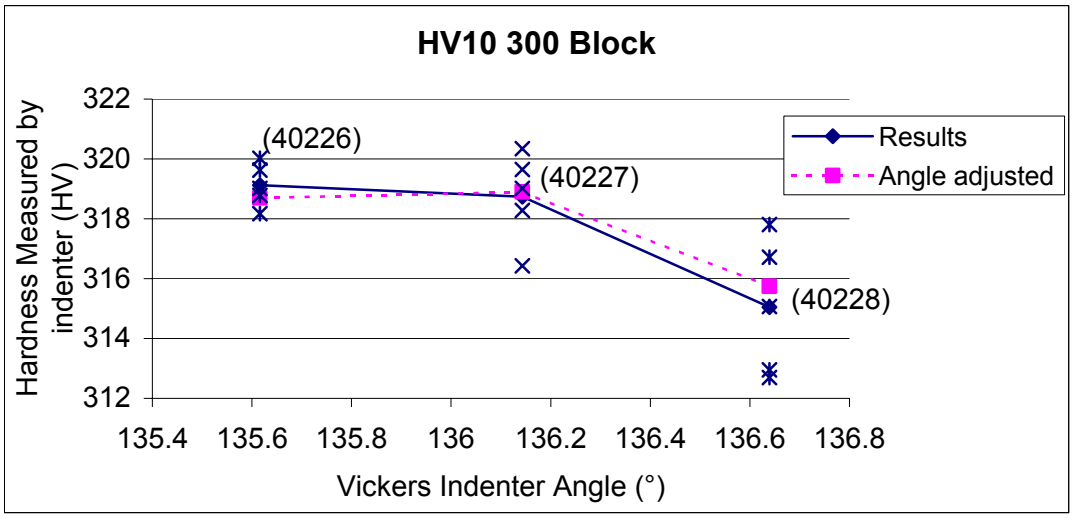

Figure 32. 300 HV10 Indenter angle against measured hardness

The angle-adjusted line is based on the measured values for the block but using the actual indenter angle within the equation used to calculate the hardness.

$$\text{Vickers Hardness} = \text{Constant} \times \frac{\text{Test Force}}{\text{Surface area of indentation}}$$

$$= 0{,}102 \frac{2F \sin \frac{136°}{2}}{d^2} \approx 0{,}1891 \frac{F}{d^2}$$

The 136° was replaced by the measured indenter angle, either 135.616° or 136.639°. This new set of readings can be seen to reduce the error caused by the indenter angle difference, levelling out the readings at 135.5°-136.5° and reducing slightly the error at 136.5°. The results seem to show that a greater effect on the measured hardness is caused by +0.5° on the 136° indenter angle.

Figure 33 displays the effective depth of the indentation measured by the laser interferometer as the depth of the indenter at the peak of force application. This has been plotted against the indenter angle, of each indenter used, to illustrate how the change affects the indentation made and hence the measured hardness.

The smaller the angle of the indenter the deeper the penetration although the surface dimensions of the indentation would vary, the 135.616° indenter creating a smaller diagonal measurement than the 136.639° indenter at an equal depth, for example. The 'Theoretical results' line indicates the gradient the line should be if all three indenters were to produce the same surface dimensions of their indentations and effectively the same hardness values for the block. This was calculated by keeping the surface dimensions and hence the hardness value constant, and basically calculating the effective depth each different indenter angle produced. This differs from the results shown which would imply that even though the 136.639° indenter penetrates the block the least the increased diagonal measurement at the block surface causes a

greater effect, giving a larger indent than the 135.616° and 136.143° indenters and hence a lower hardness value for the block.

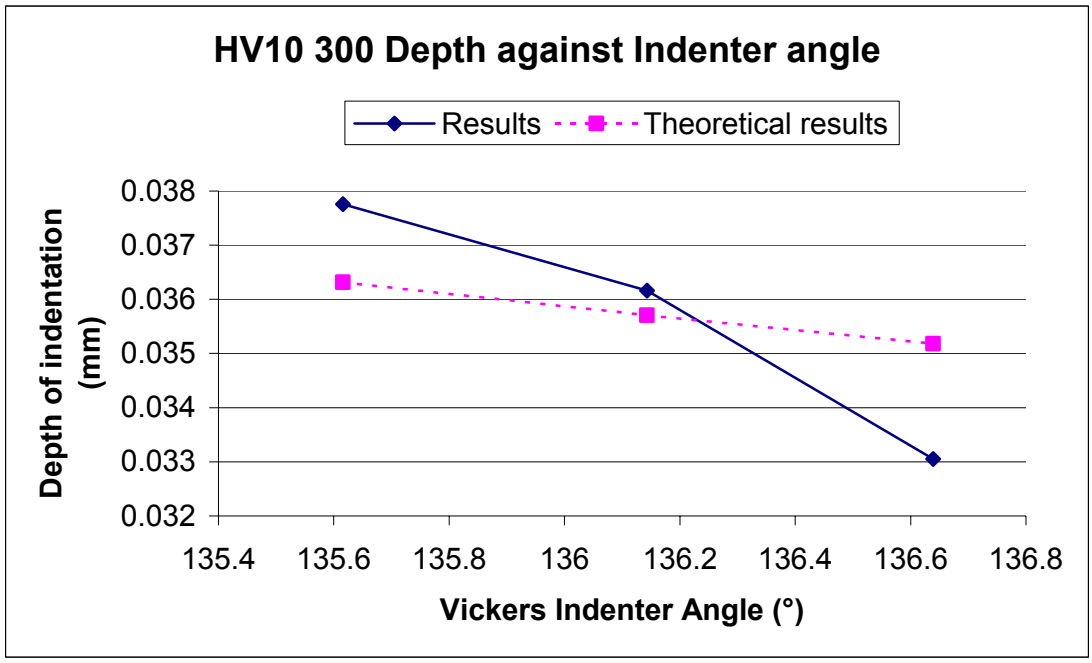

Figure 33. 300 HV10 Depth against Indenter Angle

Figure 34 like Figure 32 gives the results obtained from the three Vickers indenters but this time used with an HV10 800 block. Similarly it would appear that the indenter 40228 produces a lower hardness value than 40227, which is similar to but slightly lower than 40226.

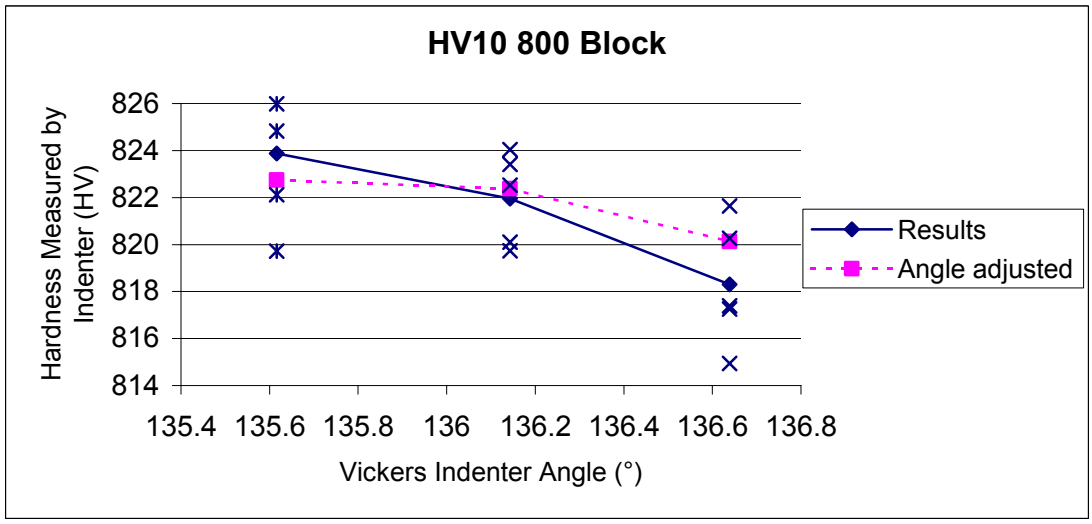

Figure 34. 800 HV10 Indenter angle against measured hardness

Figure 34, also shows the relationship between indenter angle and measured hardness on the 800 HV10 block, and the subsequent adjusted reading from inputting the actual indenter angle into the equation as in Figure 32.

The effect on the measured hardness is slightly greater on the 800 HV10 block than the 300 block, about HV 5.6 difference between the 135.616° and 136.639°, although this equates to approx 0.68 % compared to the approx 1.26 % change for the HV10 300 block. Even with the spread of the measurements, the trend is still visible, although a slight increased in this spread could account for the increased gradient.

The adjusted readings have a greater effect on the measured hardness on the harder block, reducing the range of values down to almost within 2 HV10, again the effects are more significant at reducing the difference between the standard 136° indenter on the 135.616° indenter, although the adjustment is, again, of a similar amount.

3.3.2 Rockwell C

Figure 35 gives the results obtained from the four Rockwell indenters used with a 30 HRC block. The lines plotted are based on the mean hardness value obtained with each indenter. It looks at how the difference in cone angle affects the measured readings. It would appear that the indenter 40222 and 40223 both produce harder readings then the other two indenters, both 40222 and 40223 are of a larger, roughly equal cone angle than the other indenters.

As mentioned you can separate the indenters into two groups the ~119.72° and the ~120.4° cone angled indenters. Within these two groups you can also see a difference. On both occasions the indenters with the smaller tip radius produce lower hardness value readings. As can be seen, a difference of approx 0.7° in the cone angle of the Rockwell indenter causes a change of nearly 2 HRC which is about 6.5 % of the block hardness. Looking at the difference between the two lines, the difference caused by the tip radius is also apparent. The 0.02 mm difference causes approx 0.5 Rockwell difference in the readings, with the smaller tip radius causing a greater difference in the indentation depth hence a softer hardness reading. This can bee seen more clearly in Figure 36, which also plots tip radius against measured hardness.

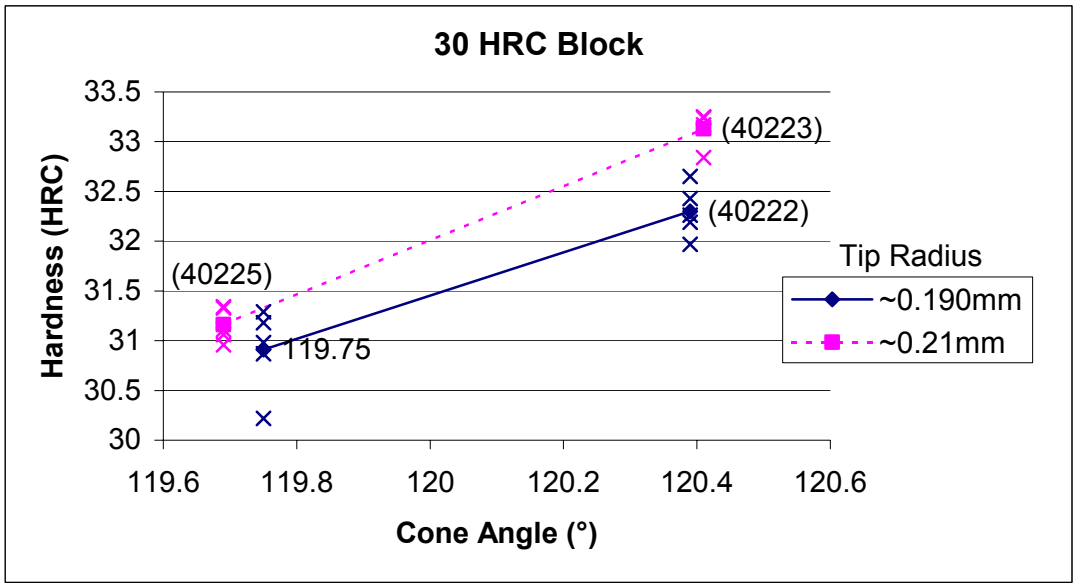

Figure 35. 30 HRC Cone angle against measured hardness

Comparing the effects of both cone angle and tip radius together is easier in Figure 36, which better illustrates the differences mentioned.

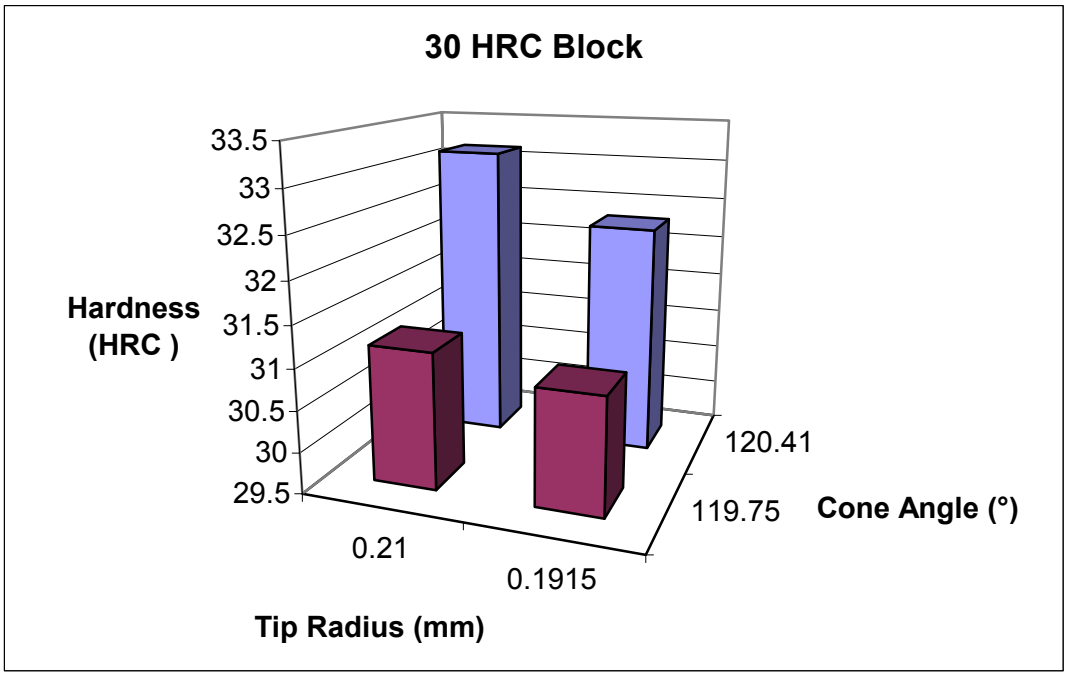

Figure 36. 30 HRC Tip radius and Cone angle against measured hardness

Figure 37, gives the results obtained from the four Rockwell indenters used with a 63 HRC block. It shows the relationships between the blocks measured hardness and cone angle and tip radius. The results for the harder 63 HRC block follow the same pattern as with the softer 30 HRC block; the larger cone angle producing a higher measured hardness and the same with a larger tip radius.

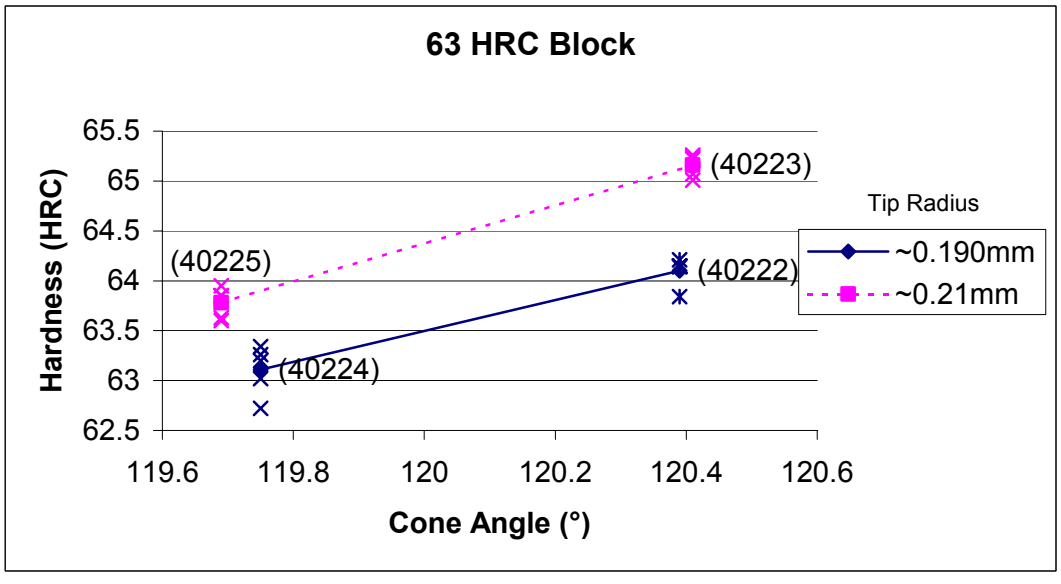

Figure 37. 63 HRC Cone angle against measured hardness

Comparing the effects of both cone angle and tip radius together is easier in Figure 38, which better illustrates the differences mentioned. It can also been seen in this figure that cone angle variation has a greater affect on the hardness value than tip radius, and that these affects seem to be greater on the softer block.

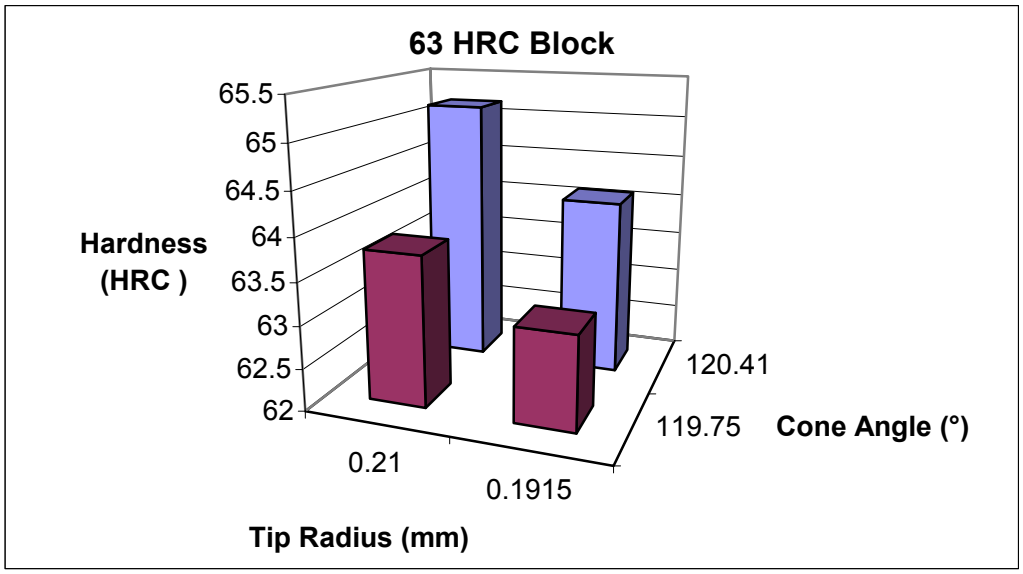

Figure 38. 63 HRC Tip radius and Cone angle against measured hardness

Figure 39 displays the results of both hardness blocks to see how the variation in hardness affects the effect caused by the change in cone angle. Cone angle was chosen as opposed to tip radius because it produced the greater variation in the measured hardness.

As can be seen in Figure 39 an increase in the hardness block, being used, of ~30 HRC reduces the effective change caused by cone angle, by between ~0.4 - 0.6 HRC.

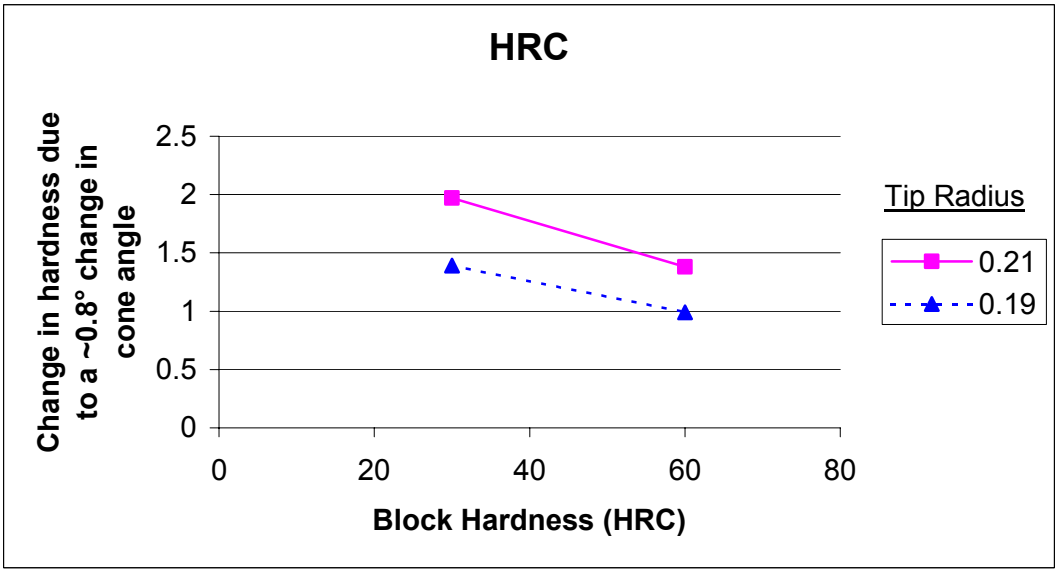

Figure 39. HRC Block hardness against change in hardness due to cone angle

4. Conclusions

Vickers: The HV10 results seem to show that there is a definite trend with increasing the indenter angle and causing the measured hardness to be reduced. This effect occurs with both hardness blocks although the effect on the measured hardness is slightly greater on the 800 HV10 block than the 300 block, about 5.6 HV difference between the results obtained from the135.54° and 136.575° indenters, although this equates to ~0.68% compared to the ~ 1.26% error for the 300 HV10 block.

It is not possible to know if the relationship between the indenter angle and apparent hardness is linear. This is the case for the harder block but the softer HV10 300 block showed a much reduced effect for the lower end of the scale. Possible further work would be needed to investigate this.

Adjusting the Vickers equation to incorporate the measured indenter angle was found to reduce the error caused especially with the 135.54° indenter. Although, again the effective change for the 136.575° indenter was not as significant and still left a relatively large error.

Leigh [40] calculated that, for a given material with the surface area of the indentation being constant, a range of 136° ±2.8° to the standard indenter angle will introduce a hardness error of less than 1%. This implies, from our results, that the surface area of the indentation is not constant as shown in Figure 34.

Although the uncertainty for these results does mask some of the effects, there still appears to be a general trend as described. Further work with a larger number of indenters could be done to understand the observed effect more, clarifying if the effects here are just due to different indenters or an actual trend caused by the differences in indenter angle and then maybe suggesting a correction factor.

Rockwell: The HRC results seem to conform to current theory and previous investigations, which have found [21] that a reduction in the tip radius results in an apparent softening of the test block, and an increase in the tip radius, results in an apparent increase.

Wood and Cotter [21] surprisingly found that a variation of ±0.35° in the cone angle did not vary the apparent hardness, which contradicts the results found here, although the results found by IMGC [28] support the results here showing the increase of cone angle increasing the apparent measured hardness while reducing the cone angle produces apparently softer hardness measurements.

The same effects to the apparent hardness, due to the variations in the indenter characteristics, were found with the harder block although the effective change in hardness due to the variation of the indenters' characteristics was reduced on the harder block. This agrees with previous work done, for example by Wood and Cotter [21] who found the effect caused by Rockwell cone angle to be reduced by a similar amount on increasing the measured hardness.

The results found seem to be more in general agreement with the practical experimentation carried out by Yamamoto and Yano [34] who reported that the

uncertainty of hardness measurement contribution due to indenter shape was of the order of ± 1 HRC. However, this uncertainty contribution was lower than the experimental data reported by Wood et al [16].

5. Acknowledgements

The authors of this report acknowledge the financial support of the National Measurement System Policy Unit of the UK Department of Trade and Industry.

6. References

[1] BS EN ISO 6506 – 1, 2, and 3 : Metallic materials – Brinell hardness test

[2] BS EN ISO 6508 – 1, 2, and 3 : Metallic materials – Rockwell hardness test

[3] BS EN ISO 6507 – 1, 2, and 3 : Metallic materials – Vickers hardness test

[4] Song J F, Smith J H, and Vorburger T V. A metrological approach to unifying Rockwell C hardness scales. Proc. 9th Int Sym of Hardness Testing in Theory and Practice. VDI Berichte, Dusseldorf, Germany, 1995, 1194, 19 – 31.

[5] Barbato G, Desogus S, and Germak A. Experimental analysis on the influence quantities in the Rockwell C hardness test. HARDMEKO '98, Beijing, China, 21-23 Sept 1998, pp 67 – 73.

[6] Barbato G, Desogus S, Germak A, Herrman K, and Polzin T. How to reach the world-wide unified scales for Rockwell hardness test with conical indenter. roc. XIV IMEKO World Congress, Tampere, Finland. 1-6 June 1997, pp 64 – 269.

[7] Low S R, Pitchure D J, and Flanigan C D. The effect of suggested changes to the Rockwell hardness test method. Proc. XVI IMEKO World Congress, Vienna, Austria. 25-28 September 2000, v III, pp 313 – 318.

[8] Barbato G, Desogus S, and Levi R. Design studies and characteristics description of the standard deadweight hardness tester of Istituto di Metrologia "G Colonnetti" (IMGC), VDI Berichte, 1978, pp 97-103.

[9] Marriner R S, and Wood J G. Comparison of international Rockwell C and Vickers HV 30 hardness scales during 1970 and 1971. NPL report MC8, 1972.

[10] Ishida H, Material deformation processes and testing conditions in the Rockwell hardness test. Proc. XIV IMEKO World Congress, Tampere, Finland. 1-6 June 1997, pp 276 – 281.

[11] Koike M, and Ishida H, Estimation of measurement uncertainty of Rockwell hardness test using orthogonal array. Proc. XV IMEKO World Congress, Osaka, Japan. 13-18 June 1999.

[12] Taguchi G, System of experimental design, UNIPUB/Kraus Int. Pub. 1987.

[13] Yamamoto H, Yamamoto T, and Minagawa T, Effects of the hardness test conditions (Importance of rigidity of indenter). Proc. XIV IMEKO World Congress, Tampere, Finland. 1-6 June 1997, pp 252 – 257.

[14] Yamamoto H, and Yamamoto T. A global standard for hardness. Proc. XV IMEKO World Congress, Osaka, Japan. 13-18 June 1999.

[15] Severn G M. Hardness testing – A survey of Vickers hardness machines, NPL report MOM C11, November 1984.

[16] Wood J G, Cotter J, and Nash P J. Hardness testing – A survey of Rockwell C scale diamond indenters, NPL report MOM 40, March 1980.

[17] Barbato G, Desogus S, and Germak A. Report on the results obtained in the comparison of the HRC scales maintained at ETCA, IMGC and MPA NRW. Rapporto Tecnico Interno R 382, IMGC, Torino 1994.

[18] Marriner R S, and Wood J G. Investigation into the measurement and performance of Rockwell C diamond indenters, Metallurgia, 87, August 1967.

[19] Barbato G, Desogus, and Germak A. The development of hardness scales in Europe. Measurement science conference, Anaheim, CA, 1992.

[20] Key P, and Soardo P. The European cooperation on calibration, testing and certification. Proc. of cooperation in metrology equivalence of the national standards dissemination of SI units, Torino, Italy, May 1992, pp. 62-85.
[21] Wood J G, and Cotter J. Performance predictions of Rockwell indenters, NPL report MOM 73, May 1985.
[22] Song J F, Low S, Pitchure D, Germak A, DeSogus S, Polzin T, Yang H Q, and Ishida H. Establishing a common Rockwell hardness scale using geometrically calibrated standard diamond indenters. Proc. XIV IMEKO World Congress, Tampere, Finland. 1-6 June 1997.
[23] Song J F, Low S, Pitchure D, Germak A, DeSogus S, Polzin T, Yang H Q, Ishida H, and Barbato G. Establishing a world-wide unified Rockwell hardness scale with metrological traceability. Metrolgia, 34, BIPM, Paris, 1997, pp 331-342.
[24] Song J F, and Vorburger T V. Standard grade Rockwell diamond indenters – A key to a worldwide unified Rockwell hardness scale. Proc. 1996 national conference of standard laboratories, NCSL, CA, 1996, 403-417.
[25] Song J F, Low S, Pitchure D, and Vorburger T V. Advances in NIST standard Rockwell diamond indenters. HARDMEKO ’98, Beijing, China, 21-23 Sept 1998, pp 61-66.
[26] Song J F, Smith J H, Vorburger T V, and Rudder F F. Stylus techniques for direct verification of Rockwell diamond indenters. VDI Berichte, Nr. 1194, 1995.
[27] Polzin T, and Schwenk D. Measurement of Rockwell indenters by laser interferometry. VDI Berichte, Nr. 1194, 1995.
[28] Barbato G, Galetto M, Germak A, and Mazzoleni F. Influence of the indenter shape in Rockwell hardness tests. HARDMEKO ’98, Beijing, China, 21-23 Sept 1998, pp 53- 59.
[29] Petik F. Factors influencing hardness measurement. OIML P 11, Paris 1983.
[30] Bochmann G, and Hild K. The influence of the deviation of indenter geometry on the hardness of Rockwell C. Zeitschrift fur Instrumentenkunde 68, S 155, 1960.
[31] Hild K. Influence of geometrical tolerances of indenters on Rockwell C hardness measurements. Zeitschrift fur Instrumentenkunde 66, S 202, 1958.
[32] Yamashiro S, and Uemura Y. Effects of test forces and indenter geometry errors on the Rockwell measurements. VDI Berichte Nr. 41, 1961, 109-121.
[33] Stepanow S S.The influence of the geometric parameters of conical indenters on the Rockwell hardness value. Trudi VNIIM 37 (97), Moskow-Leningrad, 1959, pp 106-111.
[34] Yamamoto K, and Yano H. Standardization of Rockwell C scales done by NRLM Tokyo, Bulletin NRLM series Nr 13, October 1966, pp 1-9.
[35] Pilot study on Rockwell diamond indenters. CCM-AHWGH. meeting report 1999.
[36] Song J, Low S R, and Ma L. Form error and hardness performance of Rockwell diamond indenters. Proc. XVI IMEKO World Congress, Vienna, Austria. 25-28 September 2000, v III, pp 325 – 329.
[37] Guidelines to the determination of the uncertainty of the Brinell and Vickers measuring method. PTB/5.21 note, 8.9.99.
[38] Shin S, Hida N and Yano H. Establishment of Brinell hardness and evaluation error. NRLM, Tokyo, Japan.

[39] Barbato G and Desogus S. Problems in the measurement of Vickers and Brinell indentations. Measurement, v4, No4, Oct-Dec 1986, pp137-147.
[40] Leigh I C. The micro-indentation hardness test : The practical realization of a standard. PhD thesis, University of Surrey, 1983.
[41] Tarasov L P and Thibault N W. Determination of Knoop hardness numbers independent of load. Trans Am Soc Metals. 35, 1945.
[42] Thibault N W and Nyquist H L. The measured Knoop hardness number of hard substances and factors affecting its determination. Trans Am Soc Metals. 38, 1947.
[43] Hida N and Yamamoto K. On the determination of absolute values of diagonal length of Vickers indentation. Bulletin of NRLM, No 25, Tokyo, Japan, 1970.
[44] Martins A R, Paciornik S and Pereira J A S. Brinell hardness : Image analysis and uncertainty. Proc. XVI IMEKO World Congress, Vienna, Austria. 25-28 September 2000.
[45] Stanbury G C and Davis F A, UK's provision of hardness standards. Proc. XVI IMEKO World Congress, Vienna, Austria. 25-28 September 2000, vIII, pp337-341.
[46] Stanbury G C and Davis F A, The uncertainty evaluation of NPL's hardness facility. Proc. XVI IMEKO World Congress, Vienna, Austria. 25-28 September 2000, vIII, pp331-336.
[47] Vidal AC, Caminha I and Machado RR. The manufacture of Rockwell hardness standard blocks in Brazil. Proc. XVI IMEKO World Congress, Vienna, Austria. 25-28 September 2000.
[48] Quinzhong L, Peixian Z, yuhong L, Huicai Z, and Huaxing Z. Development of hardness measurement in China. HARDMEKO '98, Beijing, China, 21-23 Sept 1998, pp 7-16.
[49] Koike M, and Ishida H. The role of hardness block in Rockwell hardness calibration system. Proc. XIV IMEKO World Congress, Tampere, Finland. 1-6 June 1997, pp 270-275.
[50] Low S R, Liggett W S, and Pitchure D J. A new method of certifying standardized Rockwell hardness test blocks. HARDMEKO '98, Beijing, China, 21-23 Sept 1998, pp 91-96.
[51] Bassett D C. The effect of ultrasonic cleaning on the hardness of metal surfaces. NPL report MOM 42, January 1984.